Specific Innate Immune Cells Uptake Fetal Antigen and Display Homeostatic Phenotypes in the Maternal Circulation

Marcia Arenas-Hernandez[1,2], Roberto Romero[1,3-7], Meyer Gershater[1,2], Li Tao[1,2], Yi Xu[1,2], Valeria Garcia-Flores[1,2], Errile Pusod[1,2], Derek Miller[1,2], Jose Galaz[1,2], Kenichiro Motomura[1,2], George Schwenkel[1,2], Robert Para[1,2], Nardhy Gomez-Lopez[1,2,8]

[1]Perinatology Research Branch, Division of Obstetrics and Maternal-Fetal Medicine, Division of Intramural Research, *Eunice Kennedy Shriver* National Institute of Child Health and Human Development, National Institutes of Health, U. S. Department of Health and Human Services, Bethesda, MD, and Detroit, MI, USA

[2]Department of Obstetrics and Gynecology, Wayne State University School of Medicine, Detroit, MI, USA

[3]Department of Obstetrics and Gynecology, University of Michigan, Ann Arbor, MI, USA.

[4]Department of Epidemiology and Biostatistics, Michigan State University, East Lansing, MI, USA

[5]Center for Molecular Medicine and Genetics, Wayne State University, Detroit, MI, USA.

[6]Detroit Medical Center, Detroit, MI, USA

[7]Department of Obstetrics and Gynecology, Florida International University, Miami, FL, USA

[8]Department of Biochemistry, Microbiology, and Immunology, Wayne State University School of Medicine, Detroit, MI, USA

Author Manuscript

This is the author manuscript accepted for publication and has undergone full peer review but has not been through the copyediting, typesetting, pagination and proofreading process, which may lead to differences between this version and the Version of Record. Please cite this article as doi: 10.1002/jlb.11051.

This article is protected by copyright. All rights reserved.

Summary Sentence: Novel interactions demonstrated between specific maternal circulating innate immune cells and fetal antigens that may contribute to the systemic mechanisms of maternal-fetal crosstalk

Running Title: Fetal antigen-carrying innate immune cells

Address correspondence to: Nardhy Gomez-Lopez, PhD, Department of Obstetrics and Gynecology, Wayne State University, School of Medicine, Perinatology Research Branch, NICHD/NIH/DHHS, 275 E Hancock St, Detroit, Michigan 48201 USA, Tel: 313-577-8904, Fax: 313-993-6769, Email: nardhy.gomez-lopez@wayne.edu; ngomezlo@med.wayne.edu

Keywords: human, innate immune cells, maternal-fetal tolerance, mice, OVA, peripheral blood, pregnancy

Author Manuscript

This article is protected by copyright. All rights reserved.

ABBREVIATIONS

APC: Antigen-presenting cell

GFP: green fluorescent protein

HLA: human leukocyte antigen

IL: interleukin

IFNγ: interferon gamma

MHC-II: major histocompatibility complex class II

NET: neutrophil extracellular trap

NK cell: natural killer cell

OVA: ovalbumin

PP: postpartum

ROS: reactive oxygen species

STBM: syncytiotrophoblast-derived microparticles

TGFβ: transforming growth factor beta

TNF: tumor necrosis factor

Author Manuscript

This article is protected by copyright. All rights reserved.

ABSTRACT

Pregnancy represents a period when the mother undergoes significant immunological changes to promote tolerance of the fetal semi-allograft. Such tolerance results from the exposure of the maternal immune system to fetal antigens, a process that has been widely investigated at the maternal-fetal interface and the adjacent draining lymph nodes. However, the peripheral mechanisms of maternal-fetal crosstalk are poorly understood. Herein, we hypothesized that specific innate immune cells interact with fetal antigens in the maternal circulation. To test this hypothesis, we utilized a mouse model of transgenic male mice that express the chicken ovalbumin (OVA) antigen under the beta-actin promoter, which were allogeneically mated with wild type females to allow for the tracking of the fetal antigen. Fetal antigen-carrying Ly6G+ and F4/80+ cells were identified in the maternal circulation, where they were more abundant in the second half of pregnancy. Such innate immune cells displayed unique phenotypes: while Ly6G+ cells expressed high levels of MHC-II and CD80 together with low levels of pro-inflammatory cytokines, F4/80+ cells upregulated the expression of CD86 as well as the anti-inflammatory cytokines IL-10 and TGFβ. *In vitro* studies using allogeneic GFP+ placental particles revealed that maternal peripheral Ly6G+ and F4/80+ cells phagocytose fetal antigens in mid and late murine pregnancy. Importantly, cytotrophoblast-derived particles were also *in vitro* engulfed by CD15+ and CD14+ cells from pregnant women, providing translational evidence that this process also occurs in humans. Collectively, this study demonstrates novel interactions between specific maternal circulating innate immune cells and fetal antigens, thereby shedding light on the systemic mechanisms of maternal-fetal crosstalk.

This article is protected by copyright. All rights reserved.

Author Manuscript

INTRODUCTION

Pregnancy represents a period of significant immunological changes in the mother that allow her to tolerate the fetal semi-allograft [1-5]. Among these adaptations, the best-characterized are those that occur at the site of contact between the maternal and fetal tissues, i.e. the maternal-fetal interface [6]. In this compartment and the adjoining tissues (e.g. the uterine-draining lymph nodes) [7-14], exposure of the maternal immune system to fetus-derived antigens initiates the establishment of tolerance [15-17] by promoting the induction of regulatory T cells (Tregs) [8, 18-27]. Other mechanisms of maternal-fetal tolerance may include effector T-cell exhaustion [28, 29] and the enrichment of the homeostatic immune microenvironment by innate immunoregulatory cells [30-37]. The placenta also contributes to local tolerance by expressing immunomodulatory non-classical MHC molecules (e.g. HLA-G) that inhibit NK cell responses [38-40] as well as inhibitory checkpoint ligands such as PD-L1 [41, 42]. Together, these and other [4, 43] cellular processes mediate the local mechanisms of maternal-fetal tolerance.

An established hallmark of pregnancy is the transfer of fetal cells into the maternal circulation [44-46] (and vice versa [47-50]), a phenomenon termed fetal or maternal microchimerism, respectively. Fetal microchimerism is detected as early as seven weeks of gestation [46], and the abundance of such cells (as well as their genetic material) steadily increase throughout pregnancy [46]. Such a process not only participates in the mechanisms of maternal-fetal tolerance [51, 52] but can also have long-lasting effects, given that fetal or maternal cells are observed in the circulation of the mother and offspring, respectively, for decades after delivery [45, 47]. In addition to fetal cells, the placenta can also release microparticles and exosomes into the maternal circulation, either due to apoptotic turnover or by active

This article is protected by copyright. All rights reserved.

Author Manuscript

103 secretion [53-63]. Specifically, placenta-derived particles serve as modulators of
104 maternal systemic immune responses [54-56, 59, 60, 64-67] and, similar to fetal
105 cells, their concentrations increase as gestation progresses [53, 56, 68]. However,
106 the interactions between placenta-derived microparticles and maternal circulating
107 immune cells have not been well explored.

108 Previous studies have established that the phenotypes and functions of
109 neutrophils and monocytes in the maternal circulation are highly impacted
110 throughout pregnancy [69-71]. Neutrophils from pregnant women exhibit an
111 enhanced state of activation as evidenced by the increased expression of cell
112 surface markers (e.g. CD14 and CD64) [69, 70], higher basal intracellular reactive
113 oxygen species (iROS) levels [69, 70, 72] and reactive oxygen metabolite release
114 [73], and altered phagocytic activity [74-76] compared to those from non-pregnant
115 women. Similarly, monocytes from pregnant women display increased cell surface
116 marker expression (e.g. CD11b, CD18 and CD64) [69, 70, 77, 78], greater basal
117 iROS production [69, 70], enhanced cytokine responses [56, 79], and perturbed
118 phagocytic activity [75, 80] compared to those from non-pregnant women. Yet,
119 whether such innate immune cells interact with fetal-derived antigens in the maternal
120 circulation is unknown.

121 The aim of this study was to investigate whether maternal circulating Ly6G+
122 cells (i.e. neutrophils) and F4/80+ cells (i.e. monocytes/macrophages) capture fetal
123 antigens throughout gestation. Specifically, we utilized transgenic male mice that
124 express the chicken ovalbumin (OVA) antigen under the beta-actin promoter, which
125 were allogeneically mated with wild type females to allow for the tracking of the fetal
126 antigen [9, 81-83]. First, we explored the localization of the fetal antigen in Ly6G+
127 and F4/80+ cells in the myometrium and periphery as well as their kinetics

This article is protected by copyright. All rights reserved.

Author Manuscript

128 throughout pregnancy. Second, using flow cytometry, we characterized the
129 phenotypes and cytokine profiles of fetal antigen-carrying Ly6G+ and F4/80+ cells
130 and confirmed their maternal origin. Third, functional *in vitro* studies were utilized to
131 investigate whether the fetal antigen can be phagocytosed by maternal peripheral
132 Ly6G+ and F4/80+ cells during mid and late murine gestation. Lastly, to demonstrate
133 the translational value of our findings in mice, we performed *in vitro* studies using
134 maternal peripheral CD15+ cells (i.e. neutrophils) and CD14+ cells (i.e. monocytes)
135 from second and third trimester pregnancies to explore whether cytotrophoblast-
136 derived particles can also be engulfed by such innate immune cells.
137

Author Manuscript

This article is protected by copyright. All rights reserved.

MATERIALS AND METHODS

Mice

C57BL/6-Tg(CAG-OVAL)916Jen/J (Act-mOVA II) (hereafter referred to as B6 CAG-OVA) male, BALB/cByJ (BALB/c) female and male, C57BL/6 female and C57BL/6 male (hereafter referred to as B6 non-CAG-OVA), C57BL/6 Actb-Egfp (GFP+) male, and DBA/2 female mice were purchased from The Jackson Laboratory (Bar Harbor, ME), bred in the animal care facility at the C.S. Mott Center for Human Growth and Development, Wayne State University, Detroit, MI, and housed under a circadian cycle (light:dark = 12:12 h). Eight- to twelve-week-old females were examined daily between 8:00 and 9:00 am for the presence of a vaginal plug, which indicated 0.5 days *post coitum* (dpc). Upon observation of vaginal plugs, female mice were removed from mating cages and housed separately. Pregnancy at 4.5 dpc was confirmed *ex vivo* by using trypan blue to stain the implantation sites, followed by washing with 1X phosphate-buffered saline (PBS; Fisher Scientific Chemicals, Fair Lawn, NJ). Pregnancy at 10.5 dpc was confirmed by a weight gain of ≥ 2 g. Postpartum BALB/c females (PP; 48 - 60 h after delivery) were also included in this study. All experiments were approved by the Institutional Animal Care and Use Committee at Wayne State University (Protocol No. A 09-08-12, A 07-03-15, 18-03-0584, and 21-04-3506).

Human subjects and clinical specimens

Human maternal peripheral blood samples were obtained at the Perinatology Research Branch, an intramural program of the *Eunice Kennedy Shriver* National Institute of Child Health and Human Development, National Institutes of Health, U.S. Department of Health and Human Services, Wayne State University (Detroit, MI),

This article is protected by copyright. All rights reserved.

Author Manuscript

and the Detroit Medical Center (Detroit, MI). The collection and use of human materials for research purposes were approved by the Institutional Review Boards of Wayne State University and the National Institute of Child Health and Human Development. All participating women provided written informed consent prior to sample collection. Samples were obtained from healthy women with normal pregnancies in the second or third trimester.

Hematoxylin & eosin staining of fetal and myometrial tissues

Fetuses and the surrounding myometrial tissues were collected from dams at 10.5 dpc, 16.5 dpc, and 18.5 dpc and placed into Tissue Tek OCT freezing medium (Sakura Finetek USA, Inc., Torrance, CA) (n = 3 - 10 each). Sagittal cuts of 16 µm thickness were taken from each fetus. Slices were mounted on slides and fixed with 4% paraformaldehyde (Electron Microscopy Sciences, Hatfield, PA) for 30 minutes (min) at 4°C. Slides were stained with hematoxylin (Thermo Fisher Scientific, Waltham, MA) for 1 min and 10 seconds (s), and immersed in clarifier for 5 s and blueing agent for 20 s, rinsing the slides with distilled water after each step. The slides were then stained with eosin (Thermo Fisher Scientific) for 45 s and dehydrated in a series of alcohol baths and xylene prior to applying coverslip. All hematoxylin & eosin (H&E) images were taken using the Vectra Polaris Multispectral Imaging System (PerkinElmer, Waltham, MA, USA) at 4x magnification.

Confocal microscopy of fetal and myometrial tissues

Fetuses and the surrounding myometrial tissues were collected from dams at 10.5 dpc, 16.5 dpc, and 18.5 dpc and placed into Tissue Tek OCT freezing medium (n = 3 - 10 each). Sagittal cuts of 16 µm thickness were taken from each fetus. Slices

This article is protected by copyright. All rights reserved.

Author Manuscript

were mounted on slides and fixed with 4% paraformaldehyde (Electron Microscopy Sciences) in 1X phosphate buffered saline (PBS; Life Technologies, Grand Island, NY) for 30 min at 4°C. Slides were then rinsed with 1X PBS (Life Technologies, Grand Island, NY), permeabilized with 0.25% Triton X-100 (Promega Corporation, Madison, WI) for 5 min at room temperature (RT), rinsed again with 1X PBS and blocked with 5% bovine serum albumin (BSA; Sigma-Aldrich, St Louis, MO) diluted in 1X PBS for 30 min at RT. The primary OVA-FITC (Cat #: 200-4233-0101, Rockland Immunochemicals, Inc. Gilbertsville, PA, USA) antibody or rabbit IgG isotype control was added and the slides were incubated for 1 h at RT. The slides were washed with 1X PBS, CD11b-Alexa Fluor 594 antibody (Cat #: 101254, BioLegend, San Diego, CA) was added, and the slides were incubated for 30 min at RT. After washing, slides were mounted with ProLong Gold Mounting medium with 4′,6-diamidino-2-phenylindole (DAPI) (Life Technologies). Immunofluorescence was visualized using a Zeiss LSM 780 laser scanning confocal microscope (Carl Zeiss Microscopy, Jena, Germany) at the Microscopy, Imaging, and Cytometry Resources Core of Wayne State University School of Medicine (https://micr.med.wayne.edu/). The 561 nm line of an "in-tune" tunable white laser was used to excite Alexa Fluor 594, the 488 nm line of the tunable white laser to excite FITC, and the 405 nm diode laser to excite DAPI.

Cell sorting

Dams at 10.5 dpc and 18.5 dpc were euthanized and peripheral blood was obtained by cardiac puncture (n = 10 each). Peripheral leukocytes were incubated with the CD16/CD32 monoclonal antibody (mAb) (FcγIII/II receptor; BD Biosciences, San Jose, CA) followed by staining using CD11b-PECF594, Ly6G-APC-Cy7 and

This article is protected by copyright. All rights reserved.

Author Manuscript

F4/80-PE mAbs (BD Biosciences), after which the cell suspensions underwent intracellular staining with either OVA-FITC antibody or rabbit IgG-FITC isotype control. Cells were resuspended in 500 µL of FACS buffer and sorted using a BD FACSAria cell sorter (BD Biosciences) and BD FACSDiva Software Version 6.1.3. The sorted CD11b+Ly6G+OVA+ or CD11b+F4/80+OVA+ cells were then resuspended with 200 µL of FACS buffer. Cytospin slides of sorted cells were prepared using Fisherbrand Superfrost microscope slides (Thermo Fisher Scientific) and a Shandon Cytospin 3 cytocentrifuge (Thermo Fisher Scientific) at 800 rpm for 5 min. After centrifugation, all slides were washed with 1X PBS and the cells were fixed with 4% paraformaldehyde for 20 min. After fixation, the slides were washed with 1X PBS, dried, and mounted using ProLong Diamond Antifade Mountant with DAPI. Images were obtained with an Olympus BX60 fluorescence microscope at 40x magnification with digital zoom.

Leukocyte isolation from the maternal peripheral blood and myometrium

Identification of fetal antigen-carrying immune cells throughout pregnancy and postpartum

Dams mated with B6 CAG-OVA or non-CAG-OVA males were euthanized at 4.5 dpc, 10.5 dpc, 16.5 dpc, 18.5 dpc, and in the postpartum period and peripheral blood was obtained by cardiac puncture. Non-pregnant females were also included as controls. Myometrial tissues from the implantation sites were collected (n = 2 – 14 each), and images of the uterine horns were taken. Isolation of leukocytes from myometrial tissues was performed as previously described [84]. Briefly, tissues were minced using fine scissors and enzymatically digested with StemPro Cell Dissociation Reagent (Life Techologies) for 35 min at 37°C. Leukocyte suspensions

This article is protected by copyright. All rights reserved.

Author Manuscript

were filtered using a 100-μm cell strainer (Fisherbrand; Fisher Scientific, Fair Lawn, NY) and washed with FACS buffer [0.1% BSA and 0.05% sodium azide (Fisher Scientific Chemicals) in 1X PBS] immediately prior to immunophenotyping.

Immunophenotyping of fetal antigen-carrying immune cells in mid and late pregnancy

Dams at 10.5 dpc (mid pregnancy) and 16.5 dpc (late pregnancy) were euthanized and peripheral blood was obtained by cardiac puncture (n = 9 – 12 each). Myometrial tissues from the implantation sites were collected (n = 9 – 11 each). Isolation of leukocytes from myometrial tissues was performed, as previously described [84]. Isolated leukocytes were utilized for immunophenotyping.

Immunophenotyping of leukocytes in the maternal peripheral blood and myometrium

Identification of fetal antigen-carrying immune cells throughout pregnancy and postpartum

Maternal peripheral blood (150 μL) and leukocyte suspensions from the myometrium were centrifuged at 1250 x g for 10 min at 4°C, and cell pellets were incubated with the CD16/CD32 mAb (FcγIII/II receptor; BD Biosciences) for 10 min, and subsequently incubated with specific fluorochrome-conjugated anti-mouse mAbs (Table S1) for 30 min at 4°C in the dark. After washing, the cells were fixed and permeabilized with the BD Cytofix/Cytoperm kit (BD Biosciences) prior to staining with intracellular Abs. For intracellular staining, OVA-FITC antibody or its isotype control (Table S1) were then added to the cells, which were then incubated for 30 min at 4°C in the dark. Following staining, cells were acquired using the BD

This article is protected by copyright. All rights reserved.

Author Manuscript

LSRFortessa flow cytometer (BD Biosciences) and FACSDiva 8.0 software (BD Biosciences). Immunophenotyping included the identification of CD45+Ly6G+OVA+ (or CD45+Ly6G+OVA-) cells and CD45+F4/80+OVA+ (or CD45+F4/80+OVA-) cells in the myometrium and peripheral blood. Data were analyzed using FlowJo software v10 (FlowJo, Ashland, OR).

Immunophenotyping of fetal antigen-carrying immune cells in mid and late pregnancy

Maternal peripheral blood (150 µL) and leukocyte suspensions from the myometrium were stained using the LIVE/DEAD Fixable Blue Dead Cell Stain Kit (Life Technologies) or Fixable Viability Stain 510 (BD Biosciences) prior to incubation with extracellular and intracellular mAbs, as described above. Immunophenotyping included the identification of surface markers (MHC-II, CD80, CD86, CD206, and CD62L) and cytokines (IFNγ, TNFα, IL-10, and TGFβ) expressed by viable CD11b+Ly6G+OVA- or CD11b+Ly6G+OVA+ cells and CD11b+F4/80+OVA- or CD11b+F4/80+OVA+ cells in the maternal peripheral blood at mid (10.5 dpc) and late (16.5 dpc) pregnancy. The expression of the same cell surface markers and cytokines were evaluated on viable CD11b+Ly6G+OVA+ cells and CD11b+F4/80+OVA+ cells in the myometrial tissues at mid (10.5 dpc) and late (16.5 dpc) pregnancy. The expression of the MHC class I molecules $H2K^b$ and $H2K^d$ was evaluated on viable CD11b+Ly6G+OVA+ and CD11b+F4/80+OVA+ cells from the maternal peripheral blood (50 µL) at mid-gestation (10.5 dpc). Data were analyzed using FlowJo software v10.

Phagocytosis assays

This article is protected by copyright. All rights reserved.

Author Manuscript

Generation of GFP+ placental particles

To obtain GFP+ placental particles, DBA/2 female mice were mated with GFP+ males and the placentas were collected at 17.5 dpc. After collection, the placentas were placed in a Petri dish with PBS and the expression of GFP was determined by *ex vivo* imaging with the IVIS Spectrum *in vivo* imaging system (PerkinElmer) [85]. An excitation filter of 465 nm and an emission filter of 520 nm were used to determine GFP expression. GFP+ placenta-derived particles were prepared using a mechanical tissue homogenizer. Whole cells and large cell fragments were removed by centrifugation at 1,000 x g for 5 min. Tissue homogenates from one placenta were divided into four aliquots, and GFP+ placenta-derived particles were collected by centrifugation at 16,000 x g for 5 min. One aliquot of placenta-derived particles was opsonized with 50 µL autologous plasma for 30 min at 37ºC and used for phagocytosis assays.

Phagocytosis of placenta-derived particles or E. coli by murine maternal peripheral Ly6G+ and F4/80+ cells

Whole blood samples were collected from pregnant C57BL/6 dams (mated with BALB/c males) at 10.5 or 16.5 dpc (n = 6 each). Whole maternal blood (50 µL) was then incubated with 10 µL of GFP+ placenta-derived particles or 10 µL of pHrodo™ Green *E. coli* BioParticles (Life Technologies) for 15 min at 37°C or on ice. After incubation, the cells were washed with FACS stain buffer (BD Biosciences) and centrifuged at 400 x g for 5 min. The cells were then incubated with anti-mouse CD11b Alexa Fluor594, anti-mouse F4/80 APC, and anti-mouse Ly6G APC-Cy7 antibodies (Table S1) in FACS staining buffer (BD Biosciences) for 30 minutes at 4°C in the dark. After incubation, erythrocytes were lysed using Ammonium-Chloride-

This article is protected by copyright. All rights reserved.

Author Manuscript

313 Potassium (ACK) lysing buffer (Lonza, Walkersville, MD), and the resulting
314 leukocytes were collected after centrifugation at 400 x g for 5 min. Finally, the cells
315 were washed and resuspended in 500 µL of FACS staining buffer and acquired
316 using the BD LSRFortessa flow cytometer and FACSDiva 9 software. The analysis
317 and figures were performed using FlowJo software version 10. The percentage of
318 active phagocytic cells was calculated as the percentage of phagocytic cells at 37°C
319 minus the percentage of phagocytic cells on ice.
320
321 *Phagocytosis of cytotrophoblast-derived particles or E. coli by human maternal*
322 *peripheral CD15+ and CD14+ cells*
323 Human peripheral blood samples were collected from healthy pregnant
324 women in the second or third trimester by venipuncture into collection tubes
325 containing EDTA (n = 4 – 6 each). Peripheral blood mononuclear cells (PBMCs) and
326 polymorphonuclear neutrophils (PMNs) were isolated using Polymorphprep™ (Alere
327 Technologies, Oslo, Norway), following the manufacturer's instructions. After
328 gradient separation, PBMCs and PMNs were washed with 1X PBS (Life
329 Technologies). Cells were resuspended in RPMI 1640 medium (Life Technologies)
330 supplemented with 5% human serum (Sigma Aldrich) and 1% penicillin/streptomycin
331 antibiotics (Life Technologies) at a concentration of 5 x 10^6 cells/mL. Swan71 human
332 first-trimester cytotrophoblast cells [86] were maintained in Dulbecco's modified
333 Eagle's medium (Life Technologies) supplemented with 10% fetal bovine serum (Life
334 Technologies) and 1% penicillin/streptomycin antibiotics. Swan71 cells were
335 collected and labeled using Vybrant® DiO cell-labeling solution (Life Technologies),
336 and then 1 X 10^7 DiO-labelled Swan71 cells were homogenized using a mechanical
337 tissue homogenizer. Whole cells and cell nuclei were removed by centrifugation at

This article is protected by copyright. All rights reserved.

Author Manuscript

2000 x g for 5 min, after which the labelled Swan71-derived particles were collected by centrifugation at 16,000 x g for 5 min. The Swan71-derived particles were opsonized with 100 µL human sera for 30 min at 37°C. Then, 5 X 10^5/100µL of combined PBMCs and PMNs were incubated with 20 µL of Swan71-derived particles or 20 µL of pHrodo™ Green *E. coli* BioParticles for 15 min at either 37°C or on ice. After incubation, the PBMCs and PMNs were washed and centrifuged at 300 x g for 5 min followed by incubation with mouse anti-human CD15 BV650 (BD Biosciences) and mouse anti-human CD14 BUV395 (BD Biosciences) antibodies in FACS staining buffer for 30 minutes at 4°C in the dark. Finally, the cells were washed and resuspended in 500 µL of FACS staining buffer and acquired using the BD LSRFortessa flow cytometer and FACSDiva 9 software. The analysis and figures were performed using FlowJo software version 10. The percentage of active phagocytic cells was calculated as the percentage of phagocytic cells at 37°C minus the percentage of phagocytic cells on ice.

Immunofluorescence and confocal microscopy of *in vitro* phagocytosis

Murine CD11b+ leukocytes were isolated from whole blood using CD11b MicroBeads (Miltenyi Biotec, San Diego, CA). Briefly, 300 µL mouse whole blood was lysed with ACK lysing buffer for 5 min on ice to remove erythrocytes. Leukocytes were collected by centrifugation at 400 x g for 5 min. CD11b+ cells were selected by isolation using CD11b MicroBeads, following the manufacturer's instructions. CD11b+ cells were placed into eight-well Lab-Tek chamber slides (Themo Fisher Scientific) with RPMI 1640 medium (Life Technologies). Chamber slides were incubated for 15 min at 37ºC. After incubation, 10 µL of GFP+ placental fragments or 10 µL pHrodo™ Green *E. coli* BioParticles were added to RPMI 1640

This article is protected by copyright. All rights reserved.

Author Manuscript

363 medium for 30 min at 37°C. Cells were then fixed with 4% paraformaldehyde and
364 immediately used for immunofluorescence staining. Next, slides were blocked using
365 Antibody Diluent/Block (PerkinElmer, Boston, MA) for 30 min at RT. Slides were then
366 incubated with rat anti-mouse CD11b Alexa Fluor 594 followed by incubation with
367 goat anti-rat IgG Alexa Fluor 594 (Table S1). Immunofluorescence signal was
368 visualized using a Zeiss LSM 780 laser scanning confocal microscope as described
369 above. Immunofluorescence signals for Alexa Fluor 647, Alexa Fluor 594, and green
370 fluorescence were excited with a 633 nm HeNe laser, a 550 nm HeNe laser, and a
371 488 nm line of multiline argon laser, respectively. The DAPI signal was excited with a
372 405 nm diode laser.

373 Maternal PBMCs and PMNs were seeded into a four-well Lab-Tek chamber
374 slide with RPMI 1640 medium supplemented with 5% human serum and 1%
375 penicillin/streptomycin antibiotics at a concentration of 5 x 10^6 cells/mL. Cells were
376 incubated for 1 h at 37°C to allow for attachment to the chamber slide. Unattached
377 cells were then removed, and new medium was added. Next, 20 µL of Swan71
378 fragments or 20 µL of pHrodo™ Green *E. coli* BioParticles were added to RPMI 1640
379 medium for 2 h at 37°C. After incubation, cells were then fixed with 4%
380 paraformaldehyde and washed with 1X PBS. Next, slides were blocked using
381 Antibody Diluent/Block (PerkinElmer, Boston, MA) for 30 min at RT. Slides were then
382 incubated with mouse anti-human CD14 (BD Biosciences) at RT for 1 h. Following
383 incubation, slides were washed with PBST [1X PBS containing 0.1% Tween 20
384 (Sigma-Aldrich)] and goat anti-mouse IgG Alexa Fluor 594 (BD Biosciences) was
385 added and incubated for 30 min at RT. Next, slides were incubated with mouse anti-
386 human CD15 Alexa Fluor 647 (BD Biosciences) for another hour at RT. Finally,
387 slides were washed and mounted with Prolong Gold Antifade Mountant with DAPI.

Author Manuscript

This article is protected by copyright. All rights reserved.

Immunofluorescence signals were visualized using a Zeiss LSM 780 laser scanning confocal microscope as described above.

Statistics

Statistical analyses were performed using SPSS v19.0 (IBM Corporation, Armonk, NY) or GraphPad Prism version 8.0.1 for Windows (GraphPad Software, San Diego, CA). The Shapiro-Wilk test was performed to determine the normality of the data. For the proportions of immune cells carrying the fetal antigen throughout pregnancy, the Shapiro-Wilk normality test was applied, after which the statistical significance between groups was determined using the Kruskal-Wallis test followed by Dunn's post-hoc test. The statistical significance between groups for the immunophenotyping at 10.5 dpc and 16.5 dpc as well as the human and murine phagocytosis experiments was determined using Mann–Whitney U-tests. A p value ≤ 0.05 was considered statistically significant.

Online Supplemental Material

Table S1. List of antibodies used for immunophenotyping and microscopy

Fig. S1. Isotype staining control for the localization of Ly6G+ and F4/80+ cells in the myometrial tissues in the second half of pregnancy

Fig. S2. Ly6G+ and F4/80+ cells in the myometrial tissues in the second half of pregnancy (OVA antibody staining control)

Author Manuscript

This article is protected by copyright. All rights reserved.

Fig. S3. Expression of OVA in maternal circulating T cells and proportions of Ly6G+ and F4/80+ cells in the myometrial tissues and maternal circulation from non-pregnant, pregnant, and post-partum dams

Fig. S4. Immunophenotyping of fetal antigen-carrying Ly6G+ and F4/80+ cells in the myometrial tissues during mid and late gestation

Fig. S5. Phagocytosis of *Escherichia coli* by murine maternal Ly6G+ or F4/80+ cells and human maternal CD15+ or CD14+ cells in the second and third trimester of pregnancy

Author Manuscript

This article is protected by copyright. All rights reserved.

RESULTS

Localization of the fetal antigen to Ly6G+ and F4/80+ cells in the myometrium and maternal circulation throughout pregnancy

Fetal antigens are released into the maternal circulation [44-46], a fraction of which are localized in the reproductive tissues [87, 88]. However, whether such antigens are found in tissue-resident innate immune cells is unknown. Herein, we first investigated the presence of the fetal antigen in Ly6G+ and F4/80+ cells residing in the myometrium surrounding the embryo using a model of B6 CAG-OVA males mated with wild type BALB/c females (Fig. 1A). The myometrial tissues surrounding the fetus and placenta were collected at 10.5 days *post coitum* (dpc), 16.5 dpc, or 18.5 dpc (Fig. 1A). H&E staining provided an anatomical overview to serve as a reference for subsequent immunofluorescence staining (Fig. 1A). Given that CD11b (a cell surface marker for cells of myeloid origin) is expressed by both monocytes and granulocytes [89-93], we evaluated the intracellular expression of the OVA protein inside CD11b+ cells in the myometrial tissues from 10.5 dpc, 16.5 dpc, and 18.5 dpc. Confocal microscopy revealed localization of the OVA protein inside of myeloid cells in the myometrium, suggesting that local innate immune cells carry the fetal antigen (Fig. 1A). Isotype staining confirmed that the visualization of the OVA protein within such cells was not due to non-specific staining (Fig. S1). To further demonstrate the specificity of the observed OVA signal in myometrial CD11b+ cells, we similarly evaluated the intracellular expression of the OVA protein in dams mated with B6 non-CAG-OVA males (Fig. S2). A positive OVA signal was not observed in myometrial CD11b+ cells from dams mated with B6 non-CAG-OVA males when using the anti-OVA antibody (Fig. S1A) or isotype control (Fig. S2B).

This article is protected by copyright. All rights reserved.

Author Manuscript

Next, we explored whether fetal antigen-carrying cells could be detected and visualized in the maternal circulation during mid-pregnancy (10.5 dpc). Ly6G+OVA+ and F4/80+OVA+ cells were detected in the maternal circulation. Intracellular immunofluorescence staining was utilized to confirm the expression of OVA in sorted innate immune cells (Fig. 1B). These findings show that innate immune cells carrying the fetal antigen are present in the myometrium and can be detected in the maternal circulation.

The local and systemic proportions of fetal antigen-carrying Ly6G+ and F4/80+ cells change throughout pregnancy

Given that the fetal antigen (OVA) was detected in Ly6G+ and F4/80+ cells in the myometrium and maternal circulation, we next investigated whether the proportions of these OVA+ cells changed throughout pregnancy. B6 CAG-OVA males were mated with wild type BALB/c (non-CAG-OVA) females, and the myometrial tissues and maternal peripheral blood were collected at 4.5 dpc (early pregnancy; Trypan blue staining was utilized to detect implantation sites), 10.5 dpc (mid pregnancy), 16.5 dpc (late pregnancy), and 18.5 dpc (term pregnancy) as well as postpartum (PP) (Fig. 2A). The populations of Ly6G+OVA+ and F4/80+OVA+ cells were determined in the myometrium and maternal circulation at each time point. The intracellular presence of OVA by CD4+ and CD8+ T cells was also examined, but these cells did not carry the fetal antigen in the maternal circulation (Fig. S3A).

The proportion of myometrial Ly6G+OVA+ cells drastically increased from 4.5 dpc to 10.5 dpc and was largely maintained until term (18.5 dpc), subsequently declining in the PP period (Fig. 2B). The proportion of myometrial F4/80+OVA+ cells peaked at 10.5 dpc and showed a slower decline from this point to PP (Fig. 2C). In

This article is protected by copyright. All rights reserved.

Author Manuscript

471 the maternal circulation, a large proportion of Ly6G+OVA+ cells was observed at
472 each time point, including PP (Fig. 2D). The proportion of peripheral Ly6G+OVA+
473 cells followed a similar trajectory to that in the myometrial tissues but with less
474 variation, gradually increasing from 4.5 dpc to 10.5 dpc and then modestly declining
475 in the PP period (Fig. 2D). In contrast, the proportion of F4/80+OVA+ cells in the
476 maternal circulation was lower than that of Ly6G+OVA+ cells at each time point, yet
477 followed an overall similar trend (Fig. 2E). To confirm the presence of OVA+ cells in
478 the myometrium and maternal circulation, we repeated the above experiment using
479 tissues obtained from dams mated with B6 non-CAG-OVA males (Fig. S3B). A
480 positive OVA signal was not detected in Ly6G+ or F4/80+ cells in the myometrial
481 tissues (Fig. S3C & D) nor in the peripheral blood (Fig. S3E & F).

482 Fetal cells are found in the maternal circulation during pregnancy and persist
483 through the post-partum period; yet, these are rare [44, 45, 47]. Therefore, we
484 confirmed the maternal origin of phagocytes carrying the OVA antigen in the
485 myometrium and peripheral blood (Fig. 3A & B). Ly6G+OVA+ and F4/80+OVA+ cells
486 in both the myometrium (Fig. 3C) and periphery (Fig. 3D) expressed $H2K^d$ (maternal
487 MHC-I haplotype) and lacked $H2K^b$ (paternal MHC-I haplotype), indicating their
488 maternal origin.

489 Together, these results indicate that the proportions of fetal antigen-carrying
490 Ly6G+ cells (neutrophils) and F4/80+ cells (monocytes/macrophages) in the
491 maternal circulation and myometrium are highest during the second half of
492 pregnancy and decline after delivery. Hereafter, we primarily focused on
493 investigating the phenotypic and functional properties of such innate immune cells in
494 the maternal circulation to further explore systemic maternal-fetal crosstalk, a poorly
495 understood phenomenon.

This article is protected by copyright. All rights reserved.

Author Manuscript

Fetal antigen-carrying Ly6G+ and F4/80+ cells in the maternal circulation display unique phenotypes

We next characterized the phenotypes of Ly6G+OVA+ and F4/80+OVA+ cells in the maternal circulation during mid and late pregnancy to determine whether these cells were distinct from their OVA- counterparts. Maternal peripheral blood was collected at 10.5 dpc and 16.5 dpc from wild type BALB/c females mated with B6 CAG-OVA males, and immunophenotyping of Ly6G+OVA+ or Ly6G+OVA- cells and F4/80+OVA+ or F4/80+OVA- cells was performed (Fig. 4A). We first examined the expression of major histocompatibility complex class II (MHC-II), an essential molecule for antigen presentation by antigen-presenting cells (APCs) [94], and found that the expression of MHC-II was significantly higher on Ly6G+OVA+ cells compared to Ly6G+OVA- cells in the maternal circulation at 10.5 dpc and tended to increase at 16.5 dpc (Fig. 4B). A similar trend was observed for the expression of MHC-II by F4/80+OVA+ cells, although this did not reach significance (Fig. 4C). We also investigated the expression of the co-stimulatory molecules CD80 and CD86 [95] by OVA+ and OVA- innate immune cells. The expression of CD80 by Ly6G+OVA+ cells was elevated in the maternal circulation (peripheral blood) compared to Ly6G+OVA- cells at both 10.5 dpc and 16.5 dpc (Fig. 4D). However, the expression of CD80 by F4/80+OVA+ cells was similar to that of F4/80+OVA- cells (Fig. 4E). Although the expression of CD86 by Ly6G+OVA+ cells did not differ from that of Ly6G+OVA- cells (Fig. 4F), the expression of this co-stimulatory molecule was increased by F4/80+OVA+ cells compared to F4/80+OVA- cells at 10.5 dpc and 16.5 dpc (Fig. 4G). No significant differences were observed in the

This article is protected by copyright. All rights reserved.

Author Manuscript

expression of the activation markers CD206 [96-99] and CD62L [100-103] by OVA+ and OVA- innate immune cells (Fig. 4H-K).

We also performed immunophenotyping of myometrial Ly6G+OVA+ and F4/80+OVA+ cells to measure expression of the molecules that were determined in OVA+ innate immune cells in the maternal circulation (Fig. S4A). Comparative analysis between OVA+ and OVA- immune cells in the myometrial tissues was not possible since very few OVA- leukocytes were found in these tissues. Therefore, we report differences between 10.5 dpc and 16.5 dpc. We found that the phenotypes of OVA+ myometrial innate immune cells differed between 10.5 dpc and 16.5 dpc (Fig. S4B-K).

Together, these data show that fetal antigen-carrying Ly6G+ cells (i.e. neutrophils) and F4/80+ cells (i.e. monocytes) display unique phenotypes in the maternal circulation.

Fetal antigen-carrying Ly6G+OVA+ and F4/80+OVA+ cells display a homeostatic cytokine profile in the maternal circulation

Next, we investigated the expression of pro-inflammatory (IFNγ and TNFα) and anti-inflammatory (IL-10 and TGFβ) cytokines by Ly6G+OVA+ or Ly6G+OVA- cells and F4/80+OVA+ or F4/80+OVA- cells. Maternal peripheral blood was collected at 10.5 dpc or 16.5 dpc from wild type BALB/c females mated with B6 CAG-OVA males, and immunophenotyping of OVA+ and OVA- neutrophils and monocytes was performed (Fig. 5A). The expression of IFNγ by Ly6G+OVA+ cells was significantly decreased compared to that of Ly6G+OVA- cells at 10.5 dpc and 16.5 dpc (Fig. 5B). Similarly, the expression of TNFα by Ly6G+OVA+ cells was reduced compared to that of Ly6G+OVA- cells at 10.5 dpc and 16.5 dpc; yet, significance was only

This article is protected by copyright. All rights reserved.

Author Manuscript

reached at 10.5 dpc (Fig. 5C). No significant differences in the expression of IL-10 and TGFβ were observed between Ly6G+OVA+ and Ly6G+OVA- cells (Fig. 5D & E). Although the expression of IFNγ and TNFα was similar between F4/80+OVA+ and F4/80+OVA- cells (Fig. 5F & G), the expression of IL-10 by F4/80+OVA+ cells was greater than that of F4/80+OVA- cells at 10.5 dpc and 16.5 dpc; yet, significance was only reached at 16.5 dpc (Fig. 5H). Interestingly, the expression of TGFβ by F4/80+OVA+ cells was greater than that of F4/80+OVA- cells at both 10.5 dpc and 16.5 dpc (Fig. 5I).

We also performed immunophenotyping of myometrial Ly6G+OVA+ and F4/80+OVA+ cells to measure expression of cytokines that were determined in OVA+ immune cells in the maternal circulation (Fig. S4A). We report that cytokine expression by OVA+ myometrial innate immune cells partially differed between 10.5 dpc and 16.5 dpc (Fig. S4L-S).

Collectively, these results suggest that fetal antigen-carrying Ly6G+ cells (i.e. neutrophils) and F4/80+ cells (i.e. monocytes) exhibit homeostatic functions in the maternal circulation by expressing low levels of pro-inflammatory cytokines or increased levels of anti-inflammatory cytokines, respectively.

Maternal circulating Ly6G+ and F4/80+ cells phagocytose placenta-derived particles in murine pregnancy

Up to this point, our results suggest that maternal innate immune cells capture the fetal antigen present in the maternal circulation. Therefore, we next investigated whether particles derived from GFP+ placentas of allogeneic pregnancies were phagocytosed by maternal peripheral Ly6G+ cells and F4/80+ cells from wild type BALB/c dams mated with B6 CAG-OVA males (Fig. 6A). Flow cytometry was utilized

This article is protected by copyright. All rights reserved.

Author Manuscript

570 to determine the phagocytosis of GFP+ placental particles (Fig. 6B). Both maternal
571 Ly6G+ and F4/80+ cells were capable of phagocytosing placenta-derived particles at
572 10.5 dpc and 16.5 dpc (Fig. 6C & D). Consistent with the similar proportions of
573 Ly6G+OVA+ and F4/80+OVA+ cells observed between 10.5 dpc and 16.5 dpc, the
574 proportion of phagocytosis did not differ between these gestational time points for
575 either cell type (Fig. 6C & D). As expected, Ly6G+ and F4/80+ cells phagocytosed *E.*
576 *coli* efficiently, which served as a positive control for phagocytosis, and again no
577 differences were observed between 10.5 dpc and 16.5 dpc (Fig. S5A-D).
578 Immunofluorescence illustrated the uptake of placenta-derived particles by maternal
579 peripheral myeloid cells (CD11b+ cells) (Fig. 6E). These data offer functional
580 evidence that maternal circulating Ly6G+ cells (i.e. neutrophils) and F4/80+ cells (i.e.
581 monocytes) can phagocytose placenta-derived particles during mid and late murine
582 gestation.
583
584 **Maternal circulating CD15+ cells and CD14+ cells phagocytose**
585 **cytotrophoblast-derived particles in human pregnancy**
586 Lastly, to demonstrate the translational value of our findings in mice, we
587 performed *in vitro* studies using maternal peripheral CD15+ (i.e. neutrophils) and
588 CD14+ (i.e. monocytes) cells from second and third trimester pregnancies to explore
589 whether cytotrophoblast-derived particles can also be engulfed by such innate
590 immune cells (Fig. 7A). Particles were derived from Swan71 cytotrophoblast cells,
591 which have been conventionally utilized for the generation of exosomes for research
592 into maternal-fetal crosstalk [61, 104, 105]. Flow cytometry was utilized to determine
593 the phagocytosis of DiO-labelled cytotrophoblast-derived particles (Fig. 7B).
594 Consistent with our findings in mice, maternal CD15+ and CD14+ cells

This article is protected by copyright. All rights reserved.

Author Manuscript

phagocytosed cytotrophoblast-derived particles during the second and third trimester (Fig. 7C & D). Such phagocytic activity appeared to be greater in the third trimester compared to the second, but this increase did not reach statistical significance (Fig. 7C & D). Immunofluorescence imaging further demonstrated the uptake of cytotrophoblast-derived particles by maternal phagocytes (Fig. 7E & F). As expected, maternal CD15+ neutrophils and CD14+ monocytes also efficiently phagocytosed *E. coli* (Fig. S5E-I). These findings provide translational value to our observations in mice by demonstrating that maternal CD15+ cells (neutrophils) and CD14+ cells (monocytes) are capable of capturing fetus-derived antigens in the maternal circulation during the second and third trimester.

Author Manuscript

This article is protected by copyright. All rights reserved.

DISCUSSION

The immune mechanisms implicated in maternal-fetal crosstalk have been extensively investigated in the uterine decidua, given that this is the primary site of interaction between the mother and the developing fetus [1-3, 5]. Another established site of maternal-fetal interaction is the intervillous space, which has primarily been studied in the context of *in utero* transmission of pathogens [106-110] and trans-placental transfer of antibodies [111-115]. Fetal antigens can also be found in the maternal circulation [17, 44, 45, 116-119], where their concentrations increase as gestation progresses [46, 85, 120-124]; however, their fate is largely unknown. Herein, we provide evidence that fetal antigens can be encountered by neutrophils and monocytes in the maternal circulation.

Neutrophils are the dominant immune cell type in the circulation and therefore play a central role in host responses in both humans and mice. Pregnant women display greater numbers of neutrophils in the circulation compared to non-pregnant women [125-128], a phenomenon that is also observed in mice [129, 130]. Yet, neutrophil numbers also vary throughout gestation [125]. A recent high-dimensional study confirmed the cellular dynamics of circulating neutrophils during normal gestation, and provided evidence of the responsiveness of these innate immune cells to a variety of stimuli [131]. Indeed, neutrophils from pregnant women possess a distinct phenotype from that of non-pregnant women, which is characterized by the enhanced expression of activation markers such as CD14 and CD64 [69, 70]. Importantly, neutrophil responsiveness towards chemotactic agents (i.e. evidence of leukocyte activation), including those derived from reproductive tissues, is increased as gestation progresses and may serve as a biomarker for pregnancy complications [71, 132-135]. Consistently, neutrophil effector functions such as ROS production

This article is protected by copyright. All rights reserved.

Author Manuscript

[69, 70, 72] and neutrophil extracellular trap (NET) formation [136] are boosted in pregnancy compared to the non-pregnant state. Regarding phagocytosis, one of the main functions of neutrophils, conflicting reports have suggested that this capability may be diminished or improved in pregnancy [74-76]. In the current study, we discovered that maternal neutrophils can phagocytose fetal antigens derived from the placenta throughout gestation. To our knowledge, this is the first demonstration that such a process occurs in the maternal circulation, providing evidence that neutrophils participate in systemic maternal-fetal crosstalk.

Fetal antigen-carrying neutrophils displayed a unique phenotype characterized by the upregulation of MHC-II and CD80, suggesting that these maternal innate immune cells exhibit APC-like functions. Previous reports have shown that non-pregnant adult neutrophils are capable of antigen presentation due to their ability to phagocytose antigens and express APC markers such as MHC-II, CD80, and CD86 [137-139]. However, dendritic cells and monocytes are superior to neutrophils in their capacity for antigen presentation [140]. Our study also demonstrated decreased expression of the pro-inflammatory cytokines IFNγ and TNFα by fetal antigen-carrying neutrophils in the maternal circulation. These data imply that, during pregnancy, circulating neutrophils exhibit anti-inflammatory functions, a phenotype that has been termed “N2” [141-143]. These results are in tandem with a previous report showing that neutrophils can exhibit homeostatic functions during mid pregnancy [144]. Yet, additional research is required to explore the contribution of neutrophils to fetal antigen presentation and tolerogenic processes in the maternal circulation.

Monocytes represent the primary subset of circulating mononuclear cells and carry out two essential functions: i) to act as sentinels in the blood vessels, and ii) to

This article is protected by copyright. All rights reserved.

Author Manuscript

transmigrate across the vessel endothelium to respond to tissue-derived signals or threats [145]. Several reports have indicated that, similar to neutrophils, circulating monocyte numbers increase throughout pregnancy [78, 126, 127, 146], although this is not consistently observed [77]. Peripheral monocytes display a gradually enhanced state of activation as gestation progresses [77, 147], indicated by elevated cytokine responses [56, 79] and phosphorylation of key signaling molecules (e.g. NF-κB) [147]. Moreover, pregnancy-derived circulating monocytes display upregulated expression of multiple activation markers such as CD11b, CD14, and CD64 [69, 70, 77, 78]. Indeed, we have recently reported that single-cell RNA sequencing-derived signatures from monocytes and macrophages are modulated in the maternal circulation throughout gestation, and such signatures are increased in women who underwent preterm labor and birth, providing a potential non-invasive biomarker for the pathological process of labor [148]. Consistent with studies of peripheral neutrophils, pregnancy has been separately reported to be associated with decreased or enhanced phagocytic function by circulating monocytes [75, 80]. Herein, we observed that peripheral monocytes are capable of engulfing placenta-derived antigens, establishing a potential mechanism whereby these innate immune cells can participate in systemic maternal-fetal interactions.

Fetal antigen-carrying monocytes exhibited a homeostatic phenotype characterized by the upregulation of CD86 together with an increased expression of TGFβ and IL-10. These findings are consistent with previous reports showing that monocytes/macrophages exhibit immunoregulatory functions during pregnancy [30, 149, 150]. Specifically, uterine macrophage populations display an alternatively activated phenotype and are involved in embryo implantation and placental development as well as in host defense [33-35, 151-154]. Yet, monocytes in the

This article is protected by copyright. All rights reserved.

Author Manuscript

maternal circulation are less characterized, and we are currently engaged in the investigation of their role during the second half of pregnancy. The systemic depletion of monocytes/macrophages induces preterm labor and birth, highlighting the homeostatic functions of these cells during pregnancy [155]. Consistently, the adoptive transfer of M2-polarized (i.e. homeostatic) macrophages prevents preterm birth in animal models of intra-amniotic inflammation [155-157]. Collectively, these data suggest that maternal peripheral monocytes display homeostatic functions during pregnancy, which include the uptake of fetal antigens released by the placenta.

It is worth mentioning that fetal antigen-carrying neutrophils and monocytes were also detected in the postpartum period (i.e. 48 - 60 hours after delivery), and such cells may continue to decline as time progresses. Yet, the presence of these cells may contribute to immunological memory [25, 26, 158-160].

A central question derived from our study concerns the events initiated in maternal neutrophils and monocytes upon fetal antigen uptake. One possibility is that maternal circulating innate immune cells phagocytose the fetal antigen for containment to prevent aberrant antigen-specific T-cell responses that could jeopardize pregnancy homeostasis. Another possibility is that maternal neutrophils and monocytes internalize the fetal antigen for processing and transport to the uterine draining lymph nodes to be presented by professional APCs, as has been previously proposed [145, 161-163], where indirect antigen presentation occurs [81]. A third possibility is that the fetal antigen is processed and presented by maternal neutrophils and monocytes to either circulating T cells or those in the lymphatic or decidual tissues. However, each of the above hypotheses require mechanistic

This article is protected by copyright. All rights reserved.

Author Manuscript

704 investigation to ascertain the fate of the fetal antigen in the maternal circulation and
705 how this process contributes to the mechanisms of maternal-fetal tolerance.

706 The current study has some limitations. The sole use of the F4/80 marker
707 does not allow us to distinguish between monocytes and macrophages; yet, it can be
708 reasonably presumed that the majority of circulating maternal OVA+ cells represent
709 monocytes, whereas those in the myometrium are primarily tissue-resident
710 macrophages. In addition, the characterization of the placenta-derived particles used
711 in the current study, as well as the mechanisms whereby these particles are
712 engulfed by maternal phagocytes, warrants further investigation in future studies.
713 Lastly, functional characterization of those maternal innate immune cells that are
714 capable of engulfing fetal antigens is required.

715 In summary, herein we provide evidence that specific maternal innate immune
716 cells are capable of fetal antigen uptake and that such cells are most prevalent in the
717 second half of murine pregnancy. These innate immune cells displayed unique
718 phenotypes: while neutrophils expressed high levels of MHC-II and CD80 together
719 with low levels of pro-inflammatory cytokines, monocytes upregulated the expression
720 of CD86 as well as the anti-inflammatory cytokines IL-10 and TGFβ. Importantly,
721 fetal antigen uptake was also displayed by neutrophils and monocytes from pregnant
722 women, providing translational evidence that this process also occurs in humans.
723 Collectively, these findings demonstrate novel interactions between specific maternal
724 circulating innate immune cells and fetal antigens, thereby shedding light on the
725 systemic mechanisms of maternal-fetal crosstalk.

Author Manuscript

This article is protected by copyright. All rights reserved.

AUTHORSHIP

M.A-H.: Investigation - Experimental Performance, Data Analysis, Writing – Original Draft, Writing – Review, Editing, and Revision.

R. R.: Investigation - Study Design & Data interpretation, Writing – Review, Editing, and Revision

M.G.: Investigation - Experimental Performance & Data Interpretation, Writing – Original Draft, Writing – Review, Editing, and Revision

L.T., Y.X., V.G-F., E.P., G.S., and R.P.: Investigation - Experimental Performance, Writing – Review, Editing, and Revision

D.M., J.G., and K.M.: Investigation, Writing – Original Draft, Writing – Review, Editing, and Revision

N.G-L.: Conceptualization, Investigation – Study Design, Writing – Original Draft, Writing – Review, Editing, and Revision

Author Manuscript

This article is protected by copyright. All rights reserved.

ACKNOWLEDGEMENTS

This research was supported by the Wayne State University Perinatal Initiative in Maternal, Perinatal and Child Health. This research was also supported, in part, by the Perinatology Research Branch, Division of Obstetrics and Maternal-Fetal Medicine, Division of Intramural Research, *Eunice Kennedy Shriver* National Institute of Child Health and Human Development, National Institutes of Health, U.S. Department of Health and Human Services (NICHD/NIH/DHHS); and, in part, with Federal funds from NICHD/NIH/DHHS under Contract No. HHSN275201300006C. The authors would like to thank Chengrui Zou and Gregorio Martinez for their assistance in carrying out some of the immunophenotyping and imaging experiments.

Dr. Romero has contributed to this work as part of his official duties as an employee of the United States Federal Government.

Author Manuscript

This article is protected by copyright. All rights reserved.

CONFLICT OF INTEREST

The authors declare no competing interests.

Author Manuscript

This article is protected by copyright. All rights reserved.

REFERENCES

1. Croy, B. A. and Murphy, S. P. Maternal-fetal immunology. *Immunol Invest* 2008; 37:389-394.
2. Chaouat, G., Petitbarat, M., Dubanchet, S., Rahmati, M., Ledee, N. Tolerance to the foetal allograft? *Am J Reprod Immunol* 2010; 63:624-636.
3. Arck, P. C. and Hecher, K. Fetomaternal immune cross-talk and its consequences for maternal and offspring's health. *Nat Med* 2013; 19:548-556.
4. Erlebacher, A. Immunology of the maternal-fetal interface. *Annu Rev Immunol* 2013; 31:387-411.
5. Bonney, E. A. Alternative theories: Pregnancy and immune tolerance. *J Reprod Immunol* 2017; 123:65-71.
6. Petroff, M. G. Immune interactions at the maternal-fetal interface. *J Reprod Immunol* 2005; 68:1-13.
7. Robertson, S. A., Guerin, L. R., Bromfield, J. J., Branson, K. M., Ahlstrom, A. C., Care, A. S. Seminal fluid drives expansion of the CD4+CD25+ T regulatory cell pool and induces tolerance to paternal alloantigens in mice. *Biol Reprod* 2009; 80:1036-1045.
8. Robertson, S. A., Guerin, L. R., Moldenhauer, L. M., Hayball, J. D. Activating T regulatory cells for tolerance in early pregnancy - the contribution of seminal fluid. *J Reprod Immunol* 2009; 83:109-116.
9. Moldenhauer, L. M., Diener, K. R., Thring, D. M., Brown, M. P., Hayball, J. D., Robertson, S. A. Cross-presentation of male seminal fluid antigens elicits T cell activation to initiate the female immune response to pregnancy. *J Immunol* 2009; 182:8080-8093.

Author Manuscript

This article is protected by copyright. All rights reserved.

10. Guerin, L. R., Moldenhauer, L. M., Prins, J. R., Bromfield, J. J., Hayball, J. D., Robertson, S. A. Seminal fluid regulates accumulation of FOXP3+ regulatory T cells in the preimplantation mouse uterus through expanding the FOXP3+ cell pool and CCL19-mediated recruitment. *Biol Reprod* 2011; 85:397-408.
11. Sharkey, D. J., Tremellen, K. P., Jasper, M. J., Gemzell-Danielsson, K., Robertson, S. A. Seminal fluid induces leukocyte recruitment and cytokine and chemokine mRNA expression in the human cervix after coitus. *J Immunol* 2012; 188:2445-2454.
12. Saito, S., Shima, T., Nakashima, A., Inada, K., Yoshino, O. Role of Paternal Antigen-Specific Treg Cells in Successful Implantation. *Am J Reprod Immunol* 2016; 75:310-316.
13. Moldenhauer, L. M., Schjenken, J. E., Hope, C. M., Green, E. S., Zhang, B., Eldi, P., Hayball, J. D., Barry, S. C., Robertson, S. A. Thymus-Derived Regulatory T Cells Exhibit Foxp3 Epigenetic Modification and Phenotype Attenuation after Mating in Mice. *J Immunol* 2019; 203:647-657.
14. Shima, T., Nakashima, A., Yasuda, I., Ushijima, A., Inada, K., Tsuda, S., Yoshino, O., Tomura, M., Saito, S. Uterine CD11c+ cells induce the development of paternal antigen-specific Tregs via seminal plasma priming. *J Reprod Immunol* 2020:103165.
15. Hill, J. A. Immunological mechanisms of pregnancy maintenance and failure: a critique of theories and therapy. *Am J Reprod Immunol* 1990; 22:33-41.
16. Tafuri, A., Alferink, J., Moller, P., Hammerling, G. J., Arnold, B. T cell awareness of paternal alloantigens during pregnancy. *Science* 1995; 270:630-633.

Author Manuscript

This article is protected by copyright. All rights reserved.

802 17. Petroff, M. G. Review: Fetal antigens--identity, origins, and influences on the
803 maternal immune system. *Placenta* 2011; 32 Suppl 2:S176-181.
804 18. Chaouat, G., Voisin, G. A., Escalier, D., Robert, P. Facilitation reaction
805 (enhancing antibodies and suppressor cells) and rejection reaction (sensitized
806 cells) from the mother to the paternal antigens of the conceptus. *Clin Exp*
807 *Immunol* 1979; 35:13-24.
808 19. Aluvihare, V. R., Kallikourdis, M., Betz, A. G. Regulatory T cells mediate
809 maternal tolerance to the fetus. *Nat Immunol* 2004; 5:266-271.
810 20. Sasaki, Y., Sakai, M., Miyazaki, S., Higuma, S., Shiozaki, A., Saito, S.
811 Decidual and peripheral blood CD4+CD25+ regulatory T cells in early
812 pregnancy subjects and spontaneous abortion cases. *Mol Hum Reprod* 2004;
813 10:347-353.
814 21. Heikkinen, J., Mottonen, M., Alanen, A., Lassila, O. Phenotypic
815 characterization of regulatory T cells in the human decidua. *Clin Exp Immunol*
816 2004; 136:373-378.
817 22. Zenclussen, A. C., Gerlof, K., Zenclussen, M. L., Sollwedel, A., Bertoja, A. Z.,
818 Ritter, T., Kotsch, K., Leber, J., Volk, H. D. Abnormal T-cell reactivity against
819 paternal antigens in spontaneous abortion: adoptive transfer of pregnancy-
820 induced CD4+CD25+ T regulatory cells prevents fetal rejection in a murine
821 abortion model. *Am J Pathol* 2005; 166:811-822.
822 23. Kahn, D. A. and Baltimore, D. Pregnancy induces a fetal antigen-specific
823 maternal T regulatory cell response that contributes to tolerance. *Proc Natl*
824 *Acad Sci U S A* 2010; 107:9299-9304.
825 24. Shima, T., Sasaki, Y., Itoh, M., Nakashima, A., Ishii, N., Sugamura, K., Saito,
826 S. Regulatory T cells are necessary for implantation and maintenance of early

This article is protected by copyright. All rights reserved.

Author Manuscript

827 pregnancy but not late pregnancy in allogeneic mice. *J Reprod Immunol* 2010;
828 85:121-129.
829 25. Samstein, R. M., Josefowicz, S. Z., Arvey, A., Treuting, P. M., Rudensky, A.
830 Y. Extrathymic generation of regulatory T cells in placental mammals
831 mitigates maternal-fetal conflict. *Cell* 2012; 150:29-38.
832 26. Rowe, J. H., Ertelt, J. M., Xin, L., Way, S. S. Pregnancy imprints regulatory
833 memory that sustains anergy to fetal antigen. *Nature* 2012; 490:102-106.
834 27. Shima, T., Inada, K., Nakashima, A., Ushijima, A., Ito, M., Yoshino, O., Saito,
835 S. Paternal antigen-specific proliferating regulatory T cells are increased in
836 uterine-draining lymph nodes just before implantation and in pregnant uterus
837 just after implantation by seminal plasma-priming in allogeneic mouse
838 pregnancy. *J Reprod Immunol* 2015; 108:72-82.
839 28. van der Zwan, A., Bi, K., Norwitz, E. R., Crespo, A. C., Claas, F. H. J.,
840 Strominger, J. L., Tilburgs, T. Mixed signature of activation and dysfunction
841 allows human decidual CD8(+) T cells to provide both tolerance and immunity.
842 *Proc Natl Acad Sci U S A* 2018; 115:385-390.
843 29. Slutsky, R., Romero, R., Xu, Y., Galaz, J., Miller, D., Done, B., Tarca, A. L.,
844 Gregor, S., Hassan, S. S., Leng, Y., Gomez-Lopez, N. Exhausted and
845 Senescent T Cells at the Maternal-Fetal Interface in Preterm and Term Labor.
846 *J Immunol Res* 2019; 2019:3128010.
847 30. Hunt, J. S., Manning, L. S., Wood, G. W. Macrophages in murine uterus are
848 immunosuppressive. *Cell Immunol* 1984; 85:499-510.
849 31. Tawfik, O. W., Hunt, J. S., Wood, G. W. Partial characterization of uterine
850 cells responsible for suppression of murine maternal anti-fetal immune
851 responses. *J Reprod Immunol* 1986; 9:213-224.

This article is protected by copyright. All rights reserved.

Author Manuscript

852 32. Gustafsson, C., Mjosberg, J., Matussek, A., Geffers, R., Matthiesen, L., Berg,
853 G., Sharma, S., Buer, J., Ernerudh, J. Gene expression profiling of human
854 decidual macrophages: evidence for immunosuppressive phenotype. *PLoS*
855 *One* 2008; 3:e2078.
856 33. Repnik, U., Tilburgs, T., Roelen, D. L., van der Mast, B. J., Kanhai, H. H.,
857 Scherjon, S., Claas, F. H. Comparison of macrophage phenotype between
858 decidua basalis and decidua parietalis by flow cytometry. *Placenta* 2008;
859 29:405-412.
860 34. Svensson, J., Jenmalm, M. C., Matussek, A., Geffers, R., Berg, G., Ernerudh,
861 J. Macrophages at the fetal-maternal interface express markers of alternative
862 activation and are induced by M-CSF and IL-10. *J Immunol* 2011; 187:3671-
863 3682.
864 35. Houser, B. L., Tilburgs, T., Hill, J., Nicotra, M. L., Strominger, J. L. Two unique
865 human decidual macrophage populations. *J Immunol* 2011; 186:2633-2642.
866 36. Miller, D., Motomura, K., Garcia-Flores, V., Romero, R., Gomez-Lopez, N.
867 Innate Lymphoid Cells in the Maternal and Fetal Compartments. *Front*
868 *Immunol* 2018; 9:2396.
869 37. Mendes, J., Areia, A. L., Rodrigues-Santos, P., Santos-Rosa, M., Mota-Pinto,
870 A. Innate Lymphoid Cells in Human Pregnancy. *Front Immunol* 2020;
871 11:551707.
872 38. Ellis, S. A., Sargent, I. L., Redman, C. W., McMichael, A. J. Evidence for a
873 novel HLA antigen found on human extravillous trophoblast and a
874 choriocarcinoma cell line. *Immunology* 1986; 59:595-601.

Author Manuscript

This article is protected by copyright. All rights reserved.

875 39. Kovats, S., Main, E. K., Librach, C., Stubblebine, M., Fisher, S. J., DeMars, R.
876 A class I antigen, HLA-G, expressed in human trophoblasts. *Science* 1990;
877 248:220-223.
878 40. Chumbley, G., King, A., Robertson, K., Holmes, N., Loke, Y. W. Resistance of
879 HLA-G and HLA-A2 transfectants to lysis by decidual NK cells. *Cell Immunol*
880 1994; 155:312-322.
881 41. Vento-Tormo, R., Efremova, M., Botting, R. A., Turco, M. Y., Vento-Tormo,
882 M., Meyer, K. B., Park, J. E., Stephenson, E., Polanski, K., Goncalves, A.,
883 Gardner, L., Holmqvist, S., Henriksson, J., Zou, A., Sharkey, A. M., Millar, B.,
884 Innes, B., Wood, L., Wilbrey-Clark, A., Payne, R. P., Ivarsson, M. A., Lisgo,
885 S., Filby, A., Rowitch, D. H., Bulmer, J. N., Wright, G. J., Stubbington, M. J. T.,
886 Haniffa, M., Moffett, A., Teichmann, S. A. Single-cell reconstruction of the
887 early maternal-fetal interface in humans. *Nature* 2018; 563:347-353.
888 42. Zhang, Y. H., Aldo, P., You, Y., Ding, J., Kaislasuo, J., Petersen, J. F.,
889 Lokkegaard, E., Peng, G., Paidas, M. J., Simpson, S., Pal, L., Guller, S., Liu,
890 H., Liao, A. H., Mor, G. Trophoblast-secreted soluble-PD-L1 modulates
891 macrophage polarization and function. *J Leukoc Biol* 2020; 108:983-998.
892 43. PrabhuDas, M., Bonney, E., Caron, K., Dey, S., Erlebacher, A., Fazleabas, A.,
893 Fisher, S., Golos, T., Matzuk, M., McCune, J. M., Mor, G., Schulz, L., Soares,
894 M., Spencer, T., Strominger, J., Way, S. S., Yoshinaga, K. Immune
895 mechanisms at the maternal-fetal interface: perspectives and challenges. *Nat*
896 *Immunol* 2015; 16:328-334.
897 44. Herzenberg, L. A., Bianchi, D. W., Schroder, J., Cann, H. M., Iverson, G. M.
898 Fetal cells in the blood of pregnant women: detection and enrichment by

Author Manuscript

This article is protected by copyright. All rights reserved.

fluorescence-activated cell sorting. *Proc Natl Acad Sci U S A* 1979; 76:1453-1455.

45. Bianchi, D. W., Zickwolf, G. K., Weil, G. J., Sylvester, S., DeMaria, M. A. Male fetal progenitor cells persist in maternal blood for as long as 27 years postpartum. *Proc Natl Acad Sci U S A* 1996; 93:705-708.

46. Ariga, H., Ohto, H., Busch, M. P., Imamura, S., Watson, R., Reed, W., Lee, T. H. Kinetics of fetal cellular and cell-free DNA in the maternal circulation during and after pregnancy: implications for noninvasive prenatal diagnosis. *Transfusion* 2001; 41:1524-1530.

47. Maloney, S., Smith, A., Furst, D. E., Myerson, D., Rupert, K., Evans, P. C., Nelson, J. L. Microchimerism of maternal origin persists into adult life. *J Clin Invest* 1999; 104:41-47.

48. Srivatsa, B., Srivatsa, S., Johnson, K. L., Bianchi, D. W. Maternal cell microchimerism in newborn tissues. *J Pediatr* 2003; 142:31-35.

49. Su, E. C., Johnson, K. L., Tighiouart, H., Bianchi, D. W. Murine maternal cell microchimerism: analysis using real-time PCR and in vivo imaging. *Biol Reprod* 2008; 78:883-887.

50. Stevens, A. M., Hermes, H. M., Kiefer, M. M., Rutledge, J. C., Nelson, J. L. Chimeric maternal cells with tissue-specific antigen expression and morphology are common in infant tissues. *Pediatr Dev Pathol* 2009; 12:337-346.

51. Kinder, J. M., Stelzer, I. A., Arck, P. C., Way, S. S. Immunological implications of pregnancy-induced microchimerism. *Nat Rev Immunol* 2017; 17:483-494.

Author Manuscript

This article is protected by copyright. All rights reserved.

922 52. Cheng, S. B., Davis, S., Sharma, S. Maternal-fetal cross talk through cell-free
923 fetal DNA, telomere shortening, microchimerism, and inflammation. *Am J*
924 *Reprod Immunol* 2018; 79:e12851.
925 53. Knight, M., Redman, C. W., Linton, E. A., Sargent, I. L. Shedding of
926 syncytiotrophoblast microvilli into the maternal circulation in pre-eclamptic
927 pregnancies. *Br J Obstet Gynaecol* 1998; 105:632-640.
928 54. Sabapatha, A., Gercel-Taylor, C., Taylor, D. D. Specific isolation of placenta-
929 derived exosomes from the circulation of pregnant women and their
930 immunoregulatory consequences. *Am J Reprod Immunol* 2006; 56:345-355.
931 55. Redman, C. W. and Sargent, I. L. Microparticles and immunomodulation in
932 pregnancy and pre-eclampsia. *J Reprod Immunol* 2007; 76:61-67.
933 56. Germain, S. J., Sacks, G. P., Sooranna, S. R., Sargent, I. L., Redman, C. W.
934 Systemic inflammatory priming in normal pregnancy and preeclampsia: the
935 role of circulating syncytiotrophoblast microparticles. *J Immunol* 2007;
936 178:5949-5956.
937 57. Burton, G. J. and Jones, C. J. Syncytial knots, sprouts, apoptosis, and
938 trophoblast deportation from the human placenta. *Taiwan J Obstet Gynecol*
939 2009; 48:28-37.
940 58. Holland, O. J., Linscheid, C., Hodes, H. C., Nauser, T. L., Gilliam, M., Stone,
941 P., Chamley, L. W., Petroff, M. G. Minor histocompatibility antigens are
942 expressed in syncytiotrophoblast and trophoblast debris: implications for
943 maternal alloreactivity to the fetus. *Am J Pathol* 2012; 180:256-266.
944 59. Stenqvist, A. C., Nagaeva, O., Baranov, V., Mincheva-Nilsson, L. Exosomes
945 secreted by human placenta carry functional Fas ligand and TRAIL molecules

Author Manuscript

This article is protected by copyright. All rights reserved.

946 and convey apoptosis in activated immune cells, suggesting exosome-
947 mediated immune privilege of the fetus. *J Immunol* 2013; 191:5515-5523.
948 60. Gohner, C., Plosch, T., Faas, M. M. Immune-modulatory effects of
949 syncytiotrophoblast extracellular vesicles in pregnancy and preeclampsia.
950 *Placenta* 2017; 60 Suppl 1:S41-S51.
951 61. Familari, M., Cronqvist, T., Masoumi, Z., Hansson, S. R. Placenta-derived
952 extracellular vesicles: their cargo and possible functions. *Reprod Fertil Dev*
953 2017; 29:433-447.
954 62. Tong, M., Abrahams, V. M., Chamley, L. W. Immunological effects of
955 placental extracellular vesicles. *Immunol Cell Biol* 2018.
956 63. Nair, S. and Salomon, C. Extracellular vesicles and their immunomodulatory
957 functions in pregnancy. *Semin Immunopathol* 2018; 40:425-437.
958 64. Reddy, A., Zhong, X. Y., Rusterholz, C., Hahn, S., Holzgreve, W., Redman, C.
959 W., Sargent, I. L. The effect of labour and placental separation on the
960 shedding of syncytiotrophoblast microparticles, cell-free DNA and mRNA in
961 normal pregnancy and pre-eclampsia. *Placenta* 2008; 29:942-949.
962 65. Kshirsagar, S. K., Alam, S. M., Jasti, S., Hodes, H., Nauser, T., Gilliam, M.,
963 Billstrand, C., Hunt, J. S., Petroff, M. G. Immunomodulatory molecules are
964 released from the first trimester and term placenta via exosomes. *Placenta*
965 2012; 33:982-990.
966 66. Tannetta, D. S., Dragovic, R. A., Gardiner, C., Redman, C. W., Sargent, I. L.
967 Characterisation of syncytiotrophoblast vesicles in normal pregnancy and pre-
968 eclampsia: expression of Flt-1 and endoglin. *PLoS One* 2013; 8:e56754.

Author Manuscript

This article is protected by copyright. All rights reserved.

969 67. Kovacs, A. F., Fekete, N., Turiak, L., Acs, A., Kohidai, L., Buzas, E. I.,
970 Pallinger, E. Unravelling the Role of Trophoblastic-Derived Extracellular
971 Vesicles in Regulatory T Cell Differentiation. *Int J Mol Sci* 2019; 20.
972 68. Tannetta, D., Collett, G., Vatish, M., Redman, C., Sargent, I.
973 Syncytiotrophoblast extracellular vesicles - Circulating biopsies reflecting
974 placental health. *Placenta* 2017; 52:134-138.
975 69. Sacks, G. P., Studena, K., Sargent, K., Redman, C. W. Normal pregnancy
976 and preeclampsia both produce inflammatory changes in peripheral blood
977 leukocytes akin to those of sepsis. *Am J Obstet Gynecol* 1998; 179:80-86.
978 70. Naccasha, N., Gervasi, M. T., Chaiworapongsa, T., Berman, S., Yoon, B. H.,
979 Maymon, E., Romero, R. Phenotypic and metabolic characteristics of
980 monocytes and granulocytes in normal pregnancy and maternal infection. *Am*
981 *J Obstet Gynecol* 2001; 185:1118-1123.
982 71. Gomez-Lopez, N., Tanaka, S., Zaeem, Z., Metz, G. A., Olson, D. M. Maternal
983 circulating leukocytes display early chemotactic responsiveness during late
984 gestation. *BMC Pregnancy Childbirth* 2013; 13 Suppl 1:S8.
985 72. Kindzelskii, A. L., Ueki, T., Michibata, H., Chaiworapongsa, T., Romero, R.,
986 Petty, H. R. 6-phosphogluconate dehydrogenase and glucose-6-phosphate
987 dehydrogenase form a supramolecular complex in human neutrophils that
988 undergoes retrograde trafficking during pregnancy. *J Immunol* 2004;
989 172:6373-6381.
990 73. Kindzelskii, A. L., Clark, A. J., Espinoza, J., Maeda, N., Aratani, Y., Romero,
991 R., Petty, H. R. Myeloperoxidase accumulates at the neutrophil surface and
992 enhances cell metabolism and oxidant release during pregnancy. *Eur J*
993 *Immunol* 2006; 36:1619-1628.

This article is protected by copyright. All rights reserved.

Author Manuscript

74. Persellin, R. H. and Thoi, L. L. Human polymorphonuclear leukocyte phagocytosis in pregnancy. Development of inhibition during gestation and recovery in the postpartum period. *Am J Obstet Gynecol* 1979; 134:250-255.

75. Lampe, R., Kover, A., Szucs, S., Pal, L., Arnyas, E., Adany, R., Poka, R. Phagocytic index of neutrophil granulocytes and monocytes in healthy and preeclamptic pregnancy. *J Reprod Immunol* 2015; 107:26-30.

76. Barriga, C., Rodriguez, A. B., Ortega, E. Increased phagocytic activity of polymorphonuclear leukocytes during pregnancy. *Eur J Obstet Gynecol Reprod Biol* 1994; 57:43-46.

77. Luppi, P., Haluszczak, C., Betters, D., Richard, C. A., Trucco, M., DeLoia, J. A. Monocytes are progressively activated in the circulation of pregnant women. *J Leukoc Biol* 2002; 72:874-884.

78. Pflitsch, C., Feldmann, C. N., Richert, L., Hagen, S., Diemert, A., Goletzke, J., Hecher, K., Jazbutyte, V., Renne, T., Arck, P. C., Altfeld, M., Ziegler, S. In-depth characterization of monocyte subsets during the course of healthy pregnancy. *J Reprod Immunol* 2020; 141:103151.

79. Sacks, G. P., Redman, C. W., Sargent, I. L. Monocytes are primed to produce the Th1 type cytokine IL-12 in normal human pregnancy: an intracellular flow cytometric analysis of peripheral blood mononuclear cells. *Clin Exp Immunol* 2003; 131:490-497.

80. Koumandakis, E., Koumandaki, I., Kaklamani, E., Sparos, L., Aravantinos, D., Trichopoulos, D. Enhanced phagocytosis of mononuclear phagocytes in pregnancy. *Br J Obstet Gynaecol* 1986; 93:1150-1154.

Author Manuscript

This article is protected by copyright. All rights reserved.

1017 81. Erlebacher, A., Vencato, D., Price, K. A., Zhang, D., Glimcher, L. H.
1018 Constraints in antigen presentation severely restrict T cell recognition of the
1019 allogeneic fetus. *J Clin Invest* 2007; 117:1399-1411.
1020 82. Moldenhauer, L. M., Hayball, J. D., Robertson, S. A. Utilising T cell receptor
1021 transgenic mice to define mechanisms of maternal T cell tolerance in
1022 pregnancy. *J Reprod Immunol* 2010; 87:1-13.
1023 83. Petroff, M. G. Review: Fetal antigens--identity, origins, and influences on the
1024 maternal immune system. *Placenta* 2011; 32 Suppl 2:S176-181.
1025 84. Arenas-Hernandez, M., Sanchez-Rodriguez, E. N., Mial, T. N., Robertson, S.
1026 A., Gomez-Lopez, N. Isolation of Leukocytes from the Murine Tissues at the
1027 Maternal-Fetal Interface. *J Vis Exp* 2015:e52866.
1028 85. Gomez-Lopez, N., Romero, R., Schwenkel, G., Garcia-Flores, V., Panaitescu,
1029 B., Varrey, A., Ayoub, F., Hassan, S. S., Phillippe, M. Cell-Free Fetal DNA
1030 Increases Prior to Labor at Term and in a Subset of Preterm Births. *Reprod*
1031 *Sci* 2020; 27:218-232.
1032 86. Straszewski-Chavez, S. L., Abrahams, V. M., Alvero, A. B., Aldo, P. B., Ma,
1033 Y., Guller, S., Romero, R., Mor, G. The isolation and characterization of a
1034 novel telomerase immortalized first trimester trophoblast cell line, Swan 71.
1035 *Placenta* 2009; 30:939-948.
1036 87. Jain, C. V., Kadam, L., van Dijk, M., Kohan-Ghadr, H. R., Kilburn, B. A.,
1037 Hartman, C., Mazzorana, V., Visser, A., Hertz, M., Bolnick, A. D., Fritz, R.,
1038 Armant, D. R., Drewlo, S. Fetal genome profiling at 5 weeks of gestation after
1039 noninvasive isolation of trophoblast cells from the endocervical canal. *Sci*
1040 *Transl Med* 2016; 8:363re364.

Author Manuscript

This article is protected by copyright. All rights reserved.

88. Moser, G., Drewlo, S., Huppertz, B., Armant, D. R. Trophoblast retrieval and isolation from the cervix: origins of cervical trophoblasts and their potential value for risk assessment of ongoing pregnancies. *Hum Reprod Update* 2018; 24:484-496.

89. Todd, R. F., 3rd, Nadler, L. M., Schlossman, S. F. Antigens on human monocytes identified by monoclonal antibodies. *J Immunol* 1981; 126:1435-1442.

90. Chen, H. M., Pahl, H. L., Scheibe, R. J., Zhang, D. E., Tenen, D. G. The Sp1 transcription factor binds the CD11b promoter specifically in myeloid cells in vivo and is essential for myeloid-specific promoter activity. *J Biol Chem* 1993; 268:8230-8239.

91. Gustafson, M. P., Lin, Y., Maas, M. L., Van Keulen, V. P., Johnston, P. B., Peikert, T., Gastineau, D. A., Dietz, A. B. A method for identification and analysis of non-overlapping myeloid immunophenotypes in humans. *PLoS One* 2015; 10:e0121546.

92. Rosen, H. and Gordon, S. Monoclonal antibody to the murine type 3 complement receptor inhibits adhesion of myelomonocytic cells in vitro and inflammatory cell recruitment in vivo. *J Exp Med* 1987; 166:1685-1701.

93. Jutila, M. A., Rott, L., Berg, E. L., Butcher, E. C. Function and regulation of the neutrophil MEL-14 antigen in vivo: comparison with LFA-1 and MAC-1. *J Immunol* 1989; 143:3318-3324.

94. Roche, P. A. and Furuta, K. The ins and outs of MHC class II-mediated antigen processing and presentation. *Nat Rev Immunol* 2015; 15:203-216.

95. Chen, L. and Flies, D. B. Molecular mechanisms of T cell co-stimulation and co-inhibition. *Nat Rev Immunol* 2013; 13:227-242.

Author Manuscript

This article is protected by copyright. All rights reserved.

96. Ezekowitz, R. A., Sastry, K., Bailly, P., Warner, A. Molecular characterization of the human macrophage mannose receptor: demonstration of multiple carbohydrate recognition-like domains and phagocytosis of yeasts in Cos-1 cells. *J Exp Med* 1990; 172:1785-1794.

97. Cuartero, M. I., Ballesteros, I., Moraga, A., Nombela, F., Vivancos, J., Hamilton, J. A., Corbi, A. L., Lizasoain, I., Moro, M. A. N2 neutrophils, novel players in brain inflammation after stroke: modulation by the PPARgamma agonist rosiglitazone. *Stroke* 2013; 44:3498-3508.

98. Nielsen, M. C., Andersen, M. N., Rittig, N., Rodgaard-Hansen, S., Gronbaek, H., Moestrup, S. K., Moller, H. J., Etzerodt, A. The macrophage-related biomarkers sCD163 and sCD206 are released by different shedding mechanisms. *J Leukoc Biol* 2019; 106:1129-1138.

99. Ono, Y., Yoshino, O., Hiraoka, T., Sato, E., Fukui, Y., Ushijima, A., Nawaz, A., Hirota, Y., Wada, S., Tobe, K., Nakashima, A., Osuga, Y., Saito, S. CD206+ M2-Like Macrophages Are Essential for Successful Implantation. *Front Immunol* 2020; 11:557184.

100. Simon, S. I., Burns, A. R., Taylor, A. D., Gopalan, P. K., Lynam, E. B., Sklar, L. A., Smith, C. W. L-selectin (CD62L) cross-linking signals neutrophil adhesive functions via the Mac-1 (CD11b/CD18) beta 2-integrin. *J Immunol* 1995; 155:1502-1514.

101. Leon, B. and Ardavin, C. Monocyte migration to inflamed skin and lymph nodes is differentially controlled by L-selectin and PSGL-1. *Blood* 2008; 111:3126-3130.

102. Bjorkman, L., Christenson, K., Davidsson, L., Martensson, J., Amirbeagi, F., Welin, A., Forsman, H., Karlsson, A., Dahlgren, C., Bylund, J. Neutrophil

This article is protected by copyright. All rights reserved.

Author Manuscript

recruitment to inflamed joints can occur without cellular priming. *J Leukoc Biol* 2019; 105:1123-1130.

103. Chadwick, J. W., Fine, N., Khoury, W., Tasevski, N., Sun, C. X., Boroumand, P., Klip, A., Glogauer, M. Tissue-specific murine neutrophil activation states in health and inflammation. *J Leukoc Biol* 2020.

104. Atay, S., Gercel-Taylor, C., Kesimer, M., Taylor, D. D. Morphologic and proteomic characterization of exosomes released by cultured extravillous trophoblast cells. *Exp Cell Res* 2011; 317:1192-1202.

105. Alam, S. M. K., Jasti, S., Kshirsagar, S. K., Tannetta, D. S., Dragovic, R. A., Redman, C. W., Sargent, I. L., Hodes, H. C., Nauser, T. L., Fortes, T., Filler, A. M., Behan, K., Martin, D. R., Fields, T. A., Petroff, B. K., Petroff, M. G. Trophoblast Glycoprotein (TPGB/5T4) in Human Placenta: Expression, Regulation, and Presence in Extracellular Microvesicles and Exosomes. *Reprod Sci* 2018; 25:185-197.

106. Delorme-Axford, E., Donker, R. B., Mouillet, J. F., Chu, T., Bayer, A., Ouyang, Y., Wang, T., Stolz, D. B., Sarkar, S. N., Morelli, A. E., Sadovsky, Y., Coyne, C. B. Human placental trophoblasts confer viral resistance to recipient cells. *Proc Natl Acad Sci U S A* 2013; 110:12048-12053.

107. Delorme-Axford, E., Bayer, A., Sadovsky, Y., Coyne, C. B. Autophagy as a mechanism of antiviral defense at the maternal-fetal interface. *Autophagy* 2013; 9:2173-2174.

108. Bayer, A., Lennemann, N. J., Ouyang, Y., Bramley, J. C., Morosky, S., Marques, E. T., Jr., Cherry, S., Sadovsky, Y., Coyne, C. B. Type III Interferons Produced by Human Placental Trophoblasts Confer Protection against Zika Virus Infection. *Cell Host Microbe* 2016; 19:705-712.

This article is protected by copyright. All rights reserved.

Author Manuscript

109. Arora, N., Sadovsky, Y., Dermody, T. S., Coyne, C. B. Microbial Vertical Transmission during Human Pregnancy. *Cell Host Microbe* 2017; 21:561-567.
110. Megli, C., Morosky, S., Rajasundaram, D., Coyne, C. B. Inflammasome signaling in human placental trophoblasts regulates immune defense against Listeria monocytogenes infection. *J Exp Med* 2021; 218.
111. Simister, N. E., Story, C. M., Chen, H. L., Hunt, J. S. An IgG-transporting Fc receptor expressed in the syncytiotrophoblast of human placenta. *Eur J Immunol* 1996; 26:1527-1531.
112. Firan, M., Bawdon, R., Radu, C., Ober, R. J., Eaken, D., Antohe, F., Ghetie, V., Ward, E. S. The MHC class I-related receptor, FcRn, plays an essential role in the maternofetal transfer of gamma-globulin in humans. *Int Immunol* 2001; 13:993-1002.
113. Radulescu, L., Antohe, F., Jinga, V., Ghetie, V., Simionescu, M. Neonatal Fc receptors discriminates and monitors the pathway of native and modified immunoglobulin G in placental endothelial cells. *Hum Immunol* 2004; 65:578-585.
114. Palmeira, P., Costa-Carvalho, B. T., Arslanian, C., Pontes, G. N., Nagao, A. T., Carneiro-Sampaio, M. M. Transfer of antibodies across the placenta and in breast milk from mothers on intravenous immunoglobulin. *Pediatr Allergy Immunol* 2009; 20:528-535.
115. Palmeira, P., Quinello, C., Silveira-Lessa, A. L., Zago, C. A., Carneiro-Sampaio, M. IgG placental transfer in healthy and pathological pregnancies. *Clin Dev Immunol* 2012; 2012:985646.

Author Manuscript

This article is protected by copyright. All rights reserved.

116. Lo, Y. M., Lo, E. S., Watson, N., Noakes, L., Sargent, I. L., Thilaganathan, B., Wainscoat, J. S. Two-way cell traffic between mother and fetus: biologic and clinical implications. *Blood* 1996; 88:4390-4395.

117. Lapaire, O., Holzgreve, W., Oosterwijk, J. C., Brinkhaus, R., Bianchi, D. W. Georg Schmorl on trophoblasts in the maternal circulation. *Placenta* 2007; 28:1-5.

118. Redman, C. W. and Sargent, I. L. Circulating microparticles in normal pregnancy and pre-eclampsia. *Placenta* 2008; 29 Suppl A:S73-77.

119. Jeanty, C., Derderian, S. C., Mackenzie, T. C. Maternal-fetal cellular trafficking: clinical implications and consequences. *Curr Opin Pediatr* 2014; 26:377-382.

120. Lo, Y. M., Corbetta, N., Chamberlain, P. F., Rai, V., Sargent, I. L., Redman, C. W., Wainscoat, J. S. Presence of fetal DNA in maternal plasma and serum. *Lancet* 1997; 350:485-487.

121. Lo, Y. M., Tein, M. S., Lau, T. K., Haines, C. J., Leung, T. N., Poon, P. M., Wainscoat, J. S., Johnson, P. J., Chang, A. M., Hjelm, N. M. Quantitative analysis of fetal DNA in maternal plasma and serum: implications for noninvasive prenatal diagnosis. *Am J Hum Genet* 1998; 62:768-775.

122. Khosrotehrani, K., Wataganara, T., Bianchi, D. W., Johnson, K. L. Fetal cell-free DNA circulates in the plasma of pregnant mice: relevance for animal models of fetomaternal trafficking. *Hum Reprod* 2004; 19:2460-2464.

123. Taglauer, E. S., Wilkins-Haug, L., Bianchi, D. W. Review: cell-free fetal DNA in the maternal circulation as an indication of placental health and disease. *Placenta* 2014; 35 Suppl:S64-68.

Author Manuscript

This article is protected by copyright. All rights reserved.

124. Herrera, C. A., Stoerker, J., Carlquist, J., Stoddard, G. J., Jackson, M., Esplin, S., Rose, N. C. Cell-free DNA, inflammation, and the initiation of spontaneous term labor. *Am J Obstet Gynecol* 2017; 217:583 e581-583 e588.

125. Belo, L., Santos-Silva, A., Rocha, S., Caslake, M., Cooney, J., Pereira-Leite, L., Quintanilha, A., Rebelo, I. Fluctuations in C-reactive protein concentration and neutrophil activation during normal human pregnancy. *Eur J Obstet Gynecol Reprod Biol* 2005; 123:46-51.

126. Veenstra van Nieuwenhoven, A. L., Bouman, A., Moes, H., Heineman, M. J., de Leij, L. F., Santema, J., Faas, M. M. Endotoxin-induced cytokine production of monocytes of third-trimester pregnant women compared with women in the follicular phase of the menstrual cycle. *Am J Obstet Gynecol* 2003; 188:1073-1077.

127. Kraus, T. A., Engel, S. M., Sperling, R. S., Kellerman, L., Lo, Y., Wallenstein, S., Escribese, M. M., Garrido, J. L., Singh, T., Loubeau, M., Moran, T. M. Characterizing the pregnancy immune phenotype: results of the viral immunity and pregnancy (VIP) study. *J Clin Immunol* 2012; 32:300-311.

128. Kostlin, N., Kugel, H., Spring, B., Leiber, A., Marme, A., Henes, M., Rieber, N., Hartl, D., Poets, C. F., Gille, C. Granulocytic myeloid derived suppressor cells expand in human pregnancy and modulate T-cell responses. *Eur J Immunol* 2014; 44:2582-2591.

129. Pan, T., Liu, Y., Zhong, L. M., Shi, M. H., Duan, X. B., Wu, K., Yang, Q., Liu, C., Wei, J. Y., Ma, X. R., Shi, K., Zhang, H., Zhou, J. Myeloid-derived suppressor cells are essential for maintaining feto-maternal immunotolerance via STAT3 signaling in mice. *J Leukoc Biol* 2016; 100:499-511.

Author Manuscript

This article is protected by copyright. All rights reserved.

130. Ostrand-Rosenberg, S., Sinha, P., Figley, C., Long, R., Park, D., Carter, D., Clements, V. K. Frontline Science: Myeloid-derived suppressor cells (MDSCs) facilitate maternal-fetal tolerance in mice. *J Leukoc Biol* 2017; 101:1091-1101.

131. Aghaeepour, N., Ganio, E. A., McIlwain, D., Tsai, A. S., Tingle, M., Van Gassen, S., Gaudilliere, D. K., Baca, Q., McNeil, L., Okada, R., Ghaemi, M. S., Furman, D., Wong, R. J., Winn, V. D., Druzin, M. L., El-Sayed, Y. Y., Quaintance, C., Gibbs, R., Darmstadt, G. L., Shaw, G. M., Stevenson, D. K., Tibshirani, R., Nolan, G. P., Lewis, D. B., Angst, M. S., Gaudilliere, B. An immune clock of human pregnancy. *Sci Immunol* 2017; 2.

132. Gomez-Lopez, N., Laresgoiti-Servitje, E., Olson, D. M., Estrada-Gutierrez, G., Vadillo-Ortega, F. The role of chemokines in term and premature rupture of the fetal membranes: a review. *Biol Reprod* 2010; 82:809-814.

133. Gomez-Lopez, N., Vadillo-Perez, L., Nessim, S., Olson, D. M., Vadillo-Ortega, F. Choriodecidua and amnion exhibit selective leukocyte chemotaxis during term human labor. *Am J Obstet Gynecol* 2011; 204:364 e369-316.

134. Gomez-Lopez, N. and Olson, D. (2012) Leukocyte activation and methods of use thereof. (USPTO, ed) The Governors of the University of Alberta, United States.

135. Gomez-Lopez, N., Tong, W. C., Arenas-Hernandez, M., Tanaka, S., Hajar, O., Olson, D. M., Taggart, M. J., Mitchell, B. F. Chemotactic activity of gestational tissues through late pregnancy, term labor, and RU486-induced preterm labor in Guinea pigs. *Am J Reprod Immunol* 2015; 73:341-352.

136. Giaglis, S., Stoikou, M., Sur Chowdhury, C., Schaefer, G., Grimolizzi, F., Rossi, S. W., Hoesli, I. M., Lapaire, O., Hasler, P., Hahn, S. Multimodal

Author Manuscript

This article is protected by copyright. All rights reserved.

Regulation of NET Formation in Pregnancy: Progesterone Antagonizes the Pro-NETotic Effect of Estrogen and G-CSF. *Front Immunol* 2016; 7:565.

137. Gosselin, E. J., Wardwell, K., Rigby, W. F., Guyre, P. M. Induction of MHC class II on human polymorphonuclear neutrophils by granulocyte/macrophage colony-stimulating factor, IFN-gamma, and IL-3. *J Immunol* 1993; 151:1482-1490.
138. Windhagen, A., Maniak, S., Gebert, A., Ferger, I., Wurster, U., Heidenreich, F. Human polymorphonuclear neutrophils express a B7-1-like molecule. *J Leukoc Biol* 1999; 66:945-952.
139. Meinderts, S. M., Baker, G., van Wijk, S., Beuger, B. M., Geissler, J., Jansen, M. H., Saris, A., Ten Brinke, A., Kuijpers, T. W., van den Berg, T. K., van Bruggen, R. Neutrophils acquire antigen-presenting cell features after phagocytosis of IgG-opsonized erythrocytes. *Blood Adv* 2019; 3:1761-1773.
140. Vono, M., Lin, A., Norrby-Teglund, A., Koup, R. A., Liang, F., Lore, K. Neutrophils acquire the capacity for antigen presentation to memory CD4(+) T cells in vitro and ex vivo. *Blood* 2017; 129:1991-2001.
141. Silvestre-Roig, C., Hidalgo, A., Soehnlein, O. Neutrophil heterogeneity: implications for homeostasis and pathogenesis. *Blood* 2016; 127:2173-2181.
142. Giese, M. A., Hind, L. E., Huttenlocher, A. Neutrophil plasticity in the tumor microenvironment. *Blood* 2019; 133:2159-2167.
143. Bouchery, T. and Harris, N. Neutrophil-macrophage cooperation and its impact on tissue repair. *Immunol Cell Biol* 2019; 97:289-298.
144. Nadkarni, S., Smith, J., Sferruzzi-Perri, A. N., Ledwozyw, A., Kishore, M., Haas, R., Mauro, C., Williams, D. J., Farsky, S. H., Marelli-Berg, F. M.,

Author Manuscript

This article is protected by copyright. All rights reserved.

Perretti, M. Neutrophils induce proangiogenic T cells with a regulatory phenotype in pregnancy. *Proc Natl Acad Sci U S A* 2016; 113:E8415-E8424.

145. Jakubzick, C. V., Randolph, G. J., Henson, P. M. Monocyte differentiation and antigen-presenting functions. *Nat Rev Immunol* 2017; 17:349-362.

146. Apps, R., Kotliarov, Y., Cheung, F., Han, K. L., Chen, J., Biancotto, A., Babyak, A., Zhou, H., Shi, R., Barnhart, L., Osgood, S. M., Belkaid, Y., Holland, S. M., Tsang, J. S., Zerbe, C. S. Multimodal immune phenotyping of maternal peripheral blood in normal human pregnancy. *JCI Insight* 2020; 5.

147. Han, X., Ghaemi, M. S., Ando, K., Peterson, L. S., Ganio, E. A., Tsai, A. S., Gaudilliere, D. K., Stelzer, I. A., Einhaus, J., Bertrand, B., Stanley, N., Culos, A., Tanada, A., Hedou, J., Tsai, E. S., Fallahzadeh, R., Wong, R. J., Judy, A. E., Winn, V. D., Druzin, M. L., Blumenfeld, Y. J., Hlatky, M. A., Quaintance, C. C., Gibbs, R. S., Carvalho, B., Shaw, G. M., Stevenson, D. K., Angst, M. S., Aghaeepour, N., Gaudilliere, B. Differential Dynamics of the Maternal Immune System in Healthy Pregnancy and Preeclampsia. *Front Immunol* 2019; 10:1305.

148. Pique-Regi, R., Romero, R., Tarca, A. L., Sendler, E. D., Xu, Y., Garcia-Flores, V., Leng, Y., Luca, F., Hassan, S. S., Gomez-Lopez, N. Single cell transcriptional signatures of the human placenta in term and preterm parturition. *Elife* 2019; 8.

149. Hunt, J. S. and Robertson, S. A. Uterine macrophages and environmental programming for pregnancy success. *J Reprod Immunol* 1996; 32:1-25.

150. Cohen, P. E., Nishimura, K., Zhu, L., Pollard, J. W. Macrophages: important accessory cells for reproductive function. *J Leukoc Biol* 1999; 66:765-772.

Author Manuscript

This article is protected by copyright. All rights reserved.

151. Care, A. S., Diener, K. R., Jasper, M. J., Brown, H. M., Ingman, W. V., Robertson, S. A. Macrophages regulate corpus luteum development during embryo implantation in mice. *J Clin Invest* 2013; 123:3472-3487.

152. Qiu, X., Zhu, L., Pollard, J. W. Colony-stimulating factor-1-dependent macrophage functions regulate the maternal decidua immune responses against Listeria monocytogenes infections during early gestation in mice. *Infect Immun* 2009; 77:85-97.

153. Svensson-Arvelund, J., Mehta, R. B., Lindau, R., Mirrasekhian, E., Rodriguez-Martinez, H., Berg, G., Lash, G. E., Jenmalm, M. C., Ernerudh, J. The human fetal placenta promotes tolerance against the semiallogeneic fetus by inducing regulatory T cells and homeostatic M2 macrophages. *J Immunol* 2015; 194:1534-1544.

154. Xu, Y., Romero, R., Miller, D., Kadam, L., Mial, T. N., Plazyo, O., Garcia-Flores, V., Hassan, S. S., Xu, Z., Tarca, A. L., Drewlo, S., Gomez-Lopez, N. An M1-like Macrophage Polarization in Decidual Tissue during Spontaneous Preterm Labor That Is Attenuated by Rosiglitazone Treatment. *J Immunol* 2016; 196:2476-2491.

155. Gomez-Lopez, N., Garcia-Flores, V., Chin, P. Y., Groome, H. M., Bijland, M. T., Diener, K. R., Romero, R., Robertson, S. A. Macrophages exert homeostatic actions in pregnancy to protect against preterm birth and fetal inflammatory injury. *JCI Insight* 2021, In Press.

156. Garcia-Flores, V., Romero, R., Schwenkel, G., Hassan, S. S., Gomez-Lopez, N. A cellular regenerative approach to prevent preterm birth: in vitro M2-polarized macrophages. *Reprod Sci* 2019; 26:74A.

Author Manuscript

This article is protected by copyright. All rights reserved.

157. Garcia-Flores, V., Romero, R., Xu, Y., Miller, D., Slutsky, R., Robertson, S., Gomez-Lopez, N. M2-polarized macrophages as a potential cell therapy to mitigate inflammation-induced preterm birth. *J Immunol* 2020; 204:145.115.

158. Gamliel, M., Goldman-Wohl, D., Isaacson, B., Gur, C., Stein, N., Yamin, R., Berger, M., Grunewald, M., Keshet, E., Rais, Y., Bornstein, C., David, E., Jelinski, A., Eisenberg, I., Greenfield, C., Ben-David, A., Imbar, T., Gilad, R., Haimov-Kochman, R., Mankuta, D., Elami-Suzin, M., Amit, I., Hanna, J. H., Yagel, S., Mandelboim, O. Trained Memory of Human Uterine NK Cells Enhances Their Function in Subsequent Pregnancies. *Immunity* 2018; 48:951-962 e955.

159. Dominguez-Andres, J. and Netea, M. G. Long-term reprogramming of the innate immune system. *J Leukoc Biol* 2019; 105:329-338.

160. Gomez-Lopez, N., Arenas-Hernandez, M., Romero, R., Miller, D., Garcia-Flores, V., Leng, Y., Xu, Y., Galaz, J., Hassan, S. S., Hsu, C. D., Tse, H., Sanchez-Torres, C., Done, B., Tarca, A. L. Regulatory T Cells Play a Role in a Subset of Idiopathic Preterm Labor/Birth and Adverse Neonatal Outcomes. *Cell Rep* 2020; 32:107874.

161. Ersland, K., Wüthrich, M., Klein, B. S. Dynamic interplay among monocyte-derived, dermal, and resident lymph node dendritic cells during the generation of vaccine immunity to fungi. *Cell Host Microbe* 2010; 7:474-487.

162. Samstein, M., Schreiber, H. A., Leiner, I. M., Susac, B., Glickman, M. S., Pamer, E. G. Essential yet limited role for CCR2$^+$ inflammatory monocytes during Mycobacterium tuberculosis-specific T cell priming. *Elife* 2013; 2:e01086.

Author Manuscript

This article is protected by copyright. All rights reserved.

163. Schreiber, H. A., Loschko, J., Karssemeijer, R. A., Escolano, A., Meredith, M. M., Mucida, D., Guermonprez, P., Nussenzweig, M. C. Intestinal monocytes and macrophages are required for T cell polarization in response to Citrobacter rodentium. *J Exp Med* 2013; 210:2025-2039.

FIGURE LEGENDS

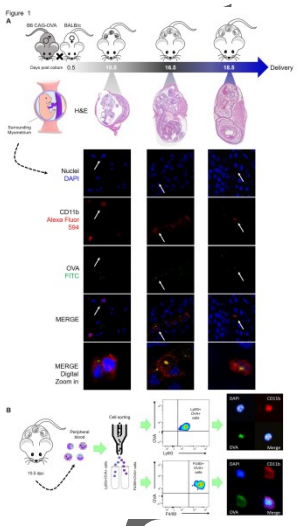

FIG. 1. Localization of the fetal antigen-carrying Ly6G+ and F4/80+ cells in the myometrial tissues and maternal circulation in the second half of pregnancy. **(A)** BALB/c females were mated with B6 CAG-OVA males, and the fetuses with surrounding myometrial tissues were collected at 10.5 days *post coitum* (dpc), 16.5 dpc, or 18.5 dpc. Representative images of the fetuses and surrounding myometrial tissues from 10.5 dpc, 16.5 dpc, and 18.5 dpc stained with hematoxylin & eosin (H&E) (4x magnification), and confocal microscopy imaging of DAPI+CD11b+OVA+

This article is protected by copyright. All rights reserved.

Author Manuscript

cells (indicated by white arrows) in the myometrial tissues (100x magnification with digital zoom) (n = 10 each). **(B)** Fluorescence-activated cell sorting (FACS) of maternal circulating CD11b+Ly6G+OVA+ and CD11b+F4/80+OVA+ cells. Representative fluorescence microscopy images of sorted Ly6G+OVA+ and F4/80+OVA+ cells. Blue = 4′,6-diamidino-2-phenylindole (DAPI), red = CD11b, green = OVA (40x magnification with digital zoom) (n = 10).

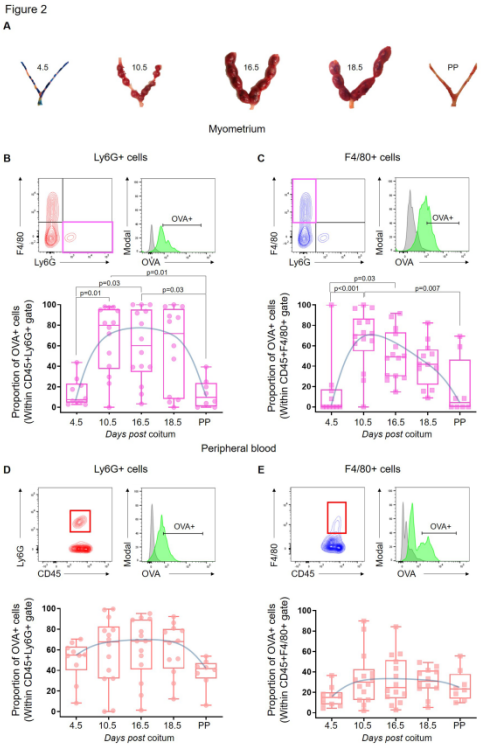

FIG. 2. Proportions of fetal antigen-carrying Ly6G+ and F4/80+ cells in the myometrial tissues and the maternal circulation throughout pregnancy. (A) Representative images of the uterine horns from BALB/c females mated with B6 CAG-OVA males at 4.5 days *post coitum* (dpc), 10.5 dpc, 16.5 dpc, or 18.5 dpc and postpartum (PP). **(B & C)** Representative gating strategies and proportions of **(B)** CD45+Ly6G+OVA+ cells and **(C)** CD45+F4/80+OVA+ cells in the myometrial tissues at 4.5 dpc, 10.5 dpc, 16.5. dpc, 18.5 dpc, and PP (n = 8 – 14 each). **(D & E)** Representative gating strategies and proportions of **(D)** CD45+Ly6G+OVA+ cells

This article is protected by copyright. All rights reserved.

and **(E)** CD45+F4/80+OVA+ cells in the maternal circulation at 4.5 dpc, 10.5 dpc, 16.5. dpc, 18.5 dpc and PP (n = 8 – 14 each). Data are shown as box-and-whisker plots where midlines indicate medians, boxes indicate interquartile ranges, and whiskers indicate minimum and maximum ranges. The p-values were determined using Kruskal-Wallis tests followed by correction for multiple comparisons ($p \leq 0.05$). Blue lines indicate changes in the trends for the proportions of Ly6G+OVA+ and F4/80+OVA+ cells throughout pregnancy.

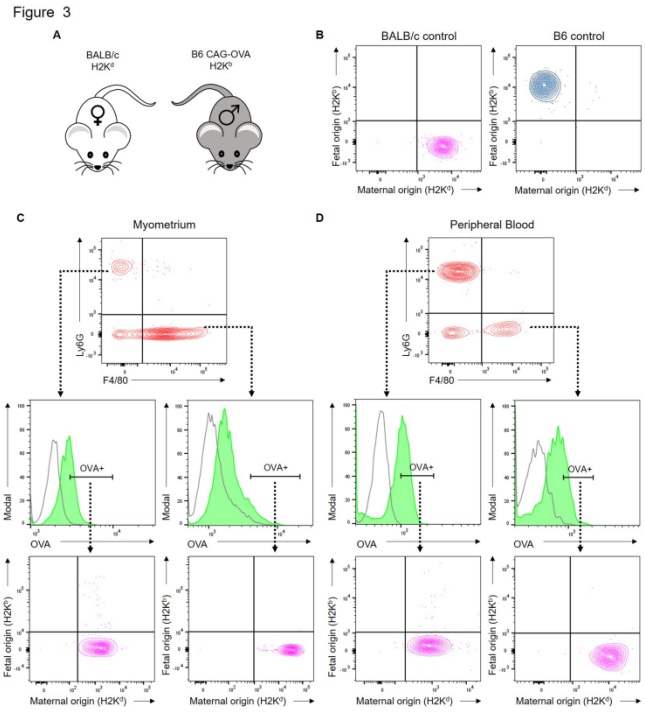

FIG. 3. Identification of MHC class I (H2K^b or H2K^d) to determine the maternal or fetal origin of Ly6G+OVA+ or F4/80+OVA+ cells in the maternal circulation and myometrium. (A) Representation of haplotypes: BALB/c females display an H2K^d haplotype and B6 CAG-OVA males display an H2K^b haplotype. **(B)** Positive BALB/c controls showing H2K^d expression and B6 controls showing H2K^b expression in the peripheral leukocytes. **(C & D)** Flow cytometry gating strategies and plots showing the expression of H2K^d haplotype, and the absence of H2K^b, confirming the maternal origin of Ly6G+OVA+ and F4/80+OVA+ cells (green

This article is protected by copyright. All rights reserved.

histograms; isotype control = grey histograms) in the myometrium and in the maternal circulation (n = 4).

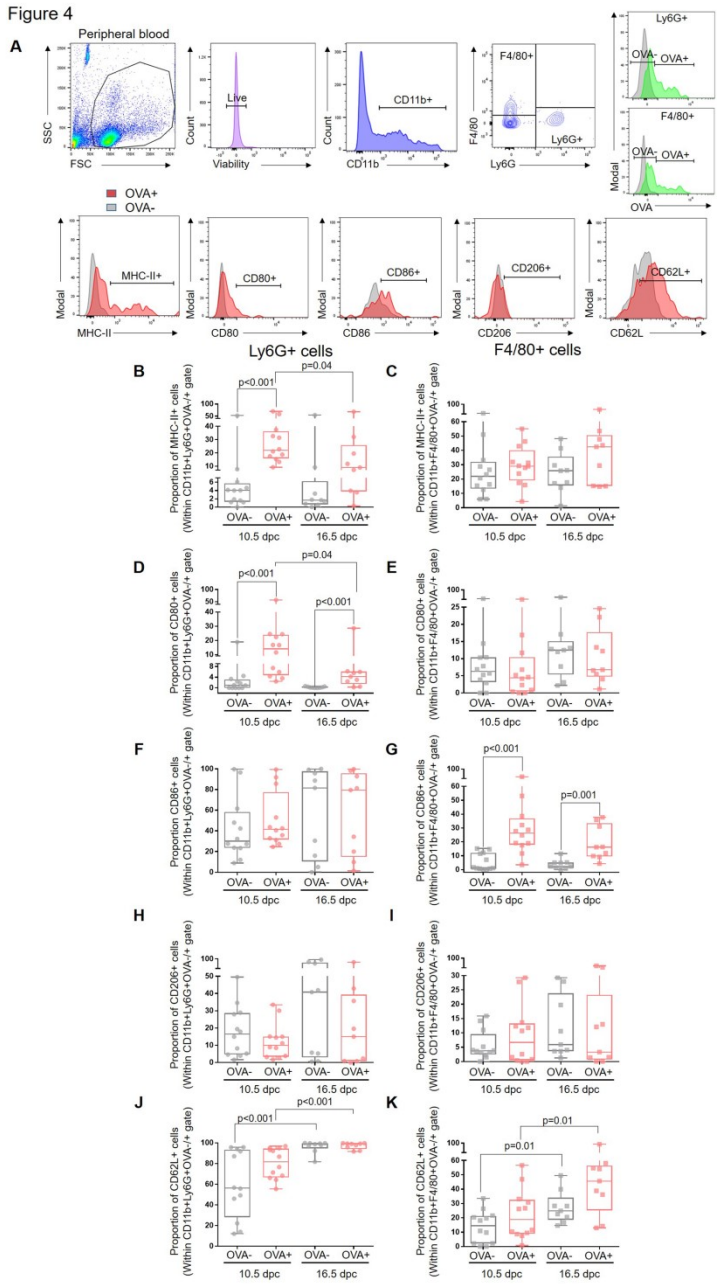

FIG. 4. Immunophenotyping of fetal antigen-carrying Ly6G+ and F4/80+ cells in the maternal circulation during mid and late gestation. (A) Flow cytometry gating strategy used to determine the Ly6G+OVA- and F4/80+OVA- cells or Ly6G+OVA+ and F4/80+OVA+ cells (green histogram = OVA; grey histogram = isotype) in the maternal circulation. Proportions of CD11b+Ly6G+OVA- (grey histograms/dots;

This article is protected by copyright. All rights reserved.

negative OVA expression) or CD11b+Ly6G+OVA+ (red histograms/dots; positive OVA expression) cells and proportions of CD11b+F4/80+OVA- (grey histograms/dots) or CD11b+F4/80+OVA+ (red histograms/dots) cells expressing **(B & C)** MHC-II, **(D & E)** CD80, **(F & G)** CD86, **(H & I)** CD206, or **(J & K)** CD62L in the maternal circulation at 10.5 days *post coitum* (dpc) and 16.5 dpc (n = 9 – 12 each). Data are shown as box-and-whisker plots where midlines indicate medians, boxes indicate interquartile ranges, and whiskers indicate minimum and maximum ranges. The p-values were determined using Mann-Whitney U-tests.

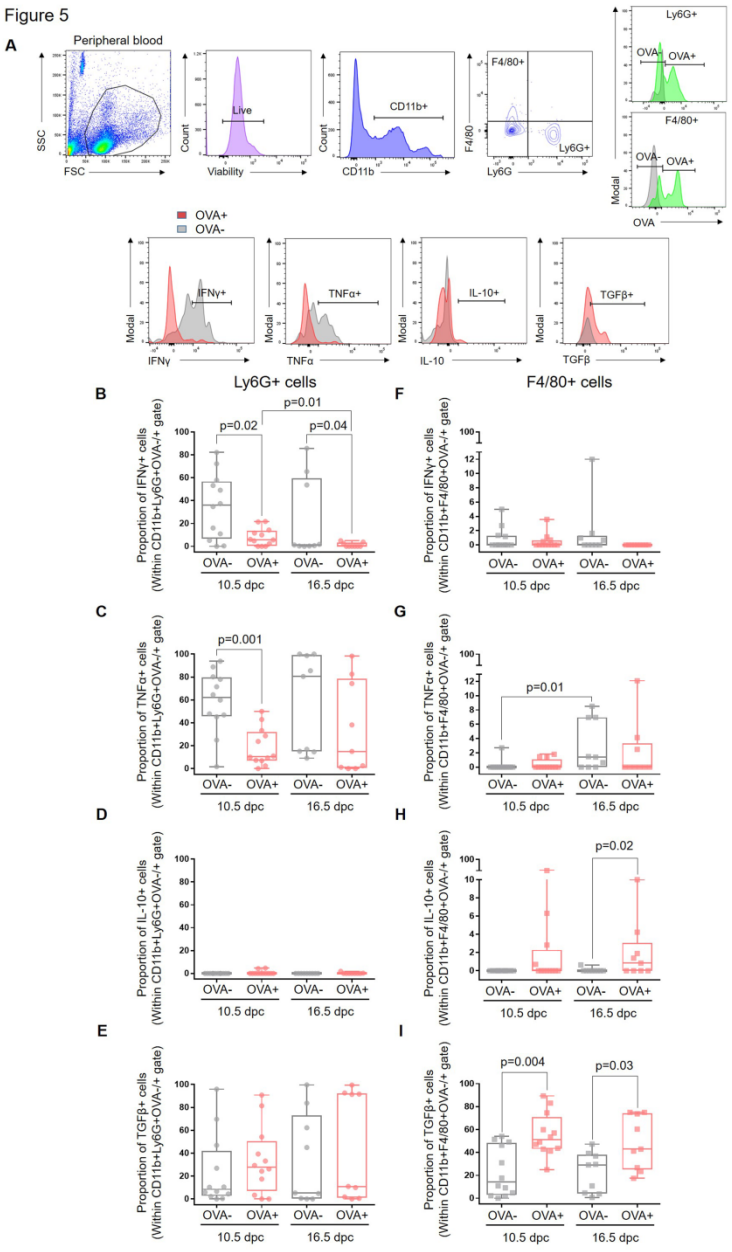

This article is protected by copyright. All rights reserved.

FIG. 5. Cytokine expression by fetal antigen-carrying Ly6G+ and F4/80+ cells in the maternal circulation during mid and late pregnancy. (A) Flow cytometry gating strategy used to determine the Ly6G+OVA- and F4/80+OVA- cells or Ly6G+OVA+ and F4/80+OVA+ cells (green histogram = OVA; grey histogram = isotype) in the maternal circulation. Proportions of CD11b+Ly6G+OVA- (grey histograms/dots; negative OVA expression) or CD11b+Ly6G+OVA+ (red histograms/dots; positive OVA expression) cells and proportions of CD11b+F4/80+OVA- (grey histograms/dots) or CD11b+F4/80+OVA+ (red histograms/dots) cells expressing **(B & F)** IFNγ, **(C & G)** TNFα, **(D & H)** IL-10, or **(E & I)** TGFβ in the maternal circulation at 10.5 days *post coitum* (dpc) and 16.5 dpc (n = 9 – 12 each). Data are shown as box-and-whisker plots where midlines indicate medians, boxes indicate interquartile ranges, and whiskers indicate minimum and maximum ranges. The p-values were determined using Mann-Whitney U-tests.

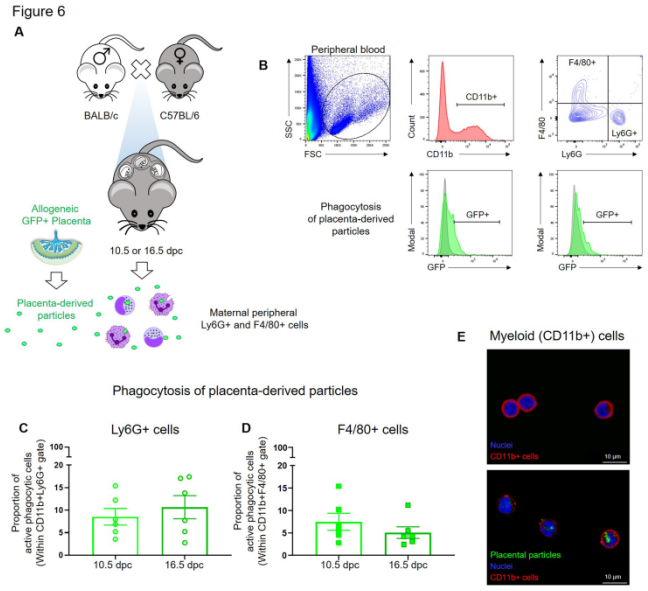

FIG. 6. Phagocytosis of placenta-derived particles by maternal Ly6G+ and F4/80+ cells in mid and late murine gestation. (A) Maternal peripheral Ly6G+ cells and F4/80+ cells were collected from wild type C57BL/6 dams mated with

This article is protected by copyright. All rights reserved.

BALB/c males at 10.5 days *post coitum* (dpc) or 16.5 dpc and cultured with placenta-derived particles from a GFP+ allogeneically-mated dam (n = 6 each). The uptake of placenta-derived particles by Ly6G+ and F4/80+ cells was evaluated by flow cytometry. **(B)** Representative gating strategy showing the uptake of GFP+ placenta-derived particles by maternal peripheral Ly6G+ and F4/80+ cells. **(C & D)** Proportions of active **(C)** Ly6G+ cells and **(D)** F4/80+ cells that phagocytosed GFP+ placenta-derived particles at 10.5 dpc or 16.5 dpc. Data are shown as scatter dot plots where bars indicate the mean and whiskers indicate the standard error of the mean. P-values were determined using Mann-Whitney U-tests. **(E)** Representative confocal microscopy images showing maternal peripheral myeloid cells (CD11b+ cells) alone (top image) or after phagocytosing GFP+ placenta-derived particles (bottom image). Blue indicates DAPI (nuclei), red indicates CD11b, and green indicates placenta-derived particles. Scale bars represent 10 μm.

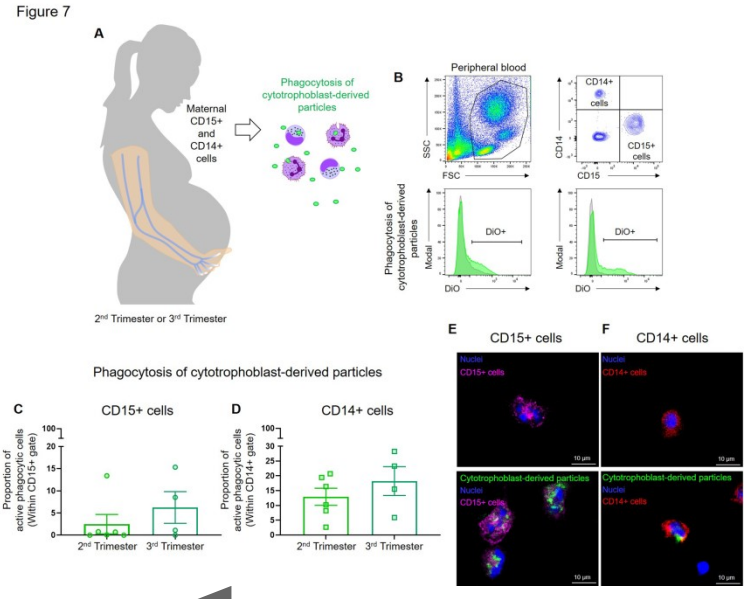

FIG. 7. Phagocytosis of cytotrophoblast-derived particles by maternal CD15+ neutrophils and CD14+ monocytes in the second and third trimester of human pregnancy. (A) Maternal peripheral CD15+ neutrophils and CD14+ monocytes were collected from pregnant women in the second or third trimester and cultured with

This article is protected by copyright. All rights reserved.

Author Manuscript

particles derived from DiO-labelled cytotrophoblast cells (n = 4 – 6 each). The uptake of cytotrophoblast-derived particles by CD15+ neutrophils and CD14+ monocytes was evaluated by flow cytometry. **(B)** Representative gating strategy showing the uptake of cytotrophoblast-derived particles by maternal peripheral CD15+ neutrophils and CD14+ monocytes. **(C & D)** Proportions of active **(C)** CD15+ neutrophils and **(D)** CD14+ monocytes that phagocytosed cytotrophoblast-derived particles in the second or third trimester. Data are shown as scatter dot plots where bars indicate the mean and whiskers indicate the standard error of the mean. P-values were determined using Mann-Whitney U-tests. **(E)** Representative confocal microscopy images showing maternal peripheral CD15+ neutrophils alone (upper image) or after phagocytosing particles derived from DiO-labelled cytotrophoblasts (bottom image). **(F)** Representative confocal microscopy images showing maternal peripheral CD14+ monocytes alone (upper image) or after phagocytosing particles derived from DiO-labelled cytotrophoblasts (bottom image). Blue immunofluorescence indicates DAPI (nuclei), pink indicates CD15, red indicates CD14, and green indicates cytotrophoblast-derived particles. Scale bars represent 10 μm.

Author Manuscript

This article is protected by copyright. All rights reserved.

1432

1433 Graphical abstract

1434

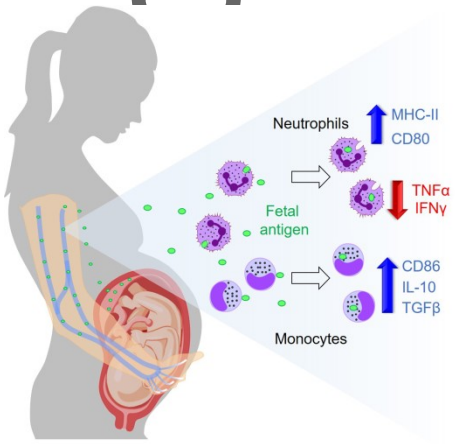

1435

Author Manuscript

This article is protected by copyright. All rights reserved.